

**A thesis submitted to the Department of Environmental Sciences and Policy of  
Central European University in partial fulfillment of the  
Degree of Master of Science**

**SEXPOT: A spatiotemporal linear programming model  
to simulate global deployment of renewable power technologies**

**Kevin UMMEL**

**May, 2011**

**Budapest**

**Erasmus Mundus Masters Course in  
Environmental Sciences, Policy and Management**

**MESPOM**



This thesis is submitted in fulfillment of the Master of Science degree awarded as a result of successful completion of the Erasmus Mundus Masters course in Environmental Sciences, Policy and Management (MESPOM) jointly operated by the University of the Aegean (Greece), Central European University (Hungary), Lund University (Sweden) and the University of Manchester (United Kingdom).

**Supported by the European Commission's Erasmus Mundus Programme**



Education and Culture

**Erasmus Mundus**

## **COPYRIGHT AND OWNERSHIP**

(1) Copyright in text of this thesis rests with the Author. Copies (by any process) either in full, or of extracts, may be made only in accordance with instructions given by the Author and lodged in the Central European University Library. Details may be obtained from the Librarian. This page must form part of any such copies made. Further copies (by any process) of copies made in accordance with such instructions may not be made without the permission (in writing) of the Author.

(2) The ownership of any intellectual property rights which may be described in this thesis is vested in the Central European University, subject to any prior agreement to the contrary, and may not be made available for use by third parties without the written permission of the University, which will prescribe the terms and conditions of any such agreement.

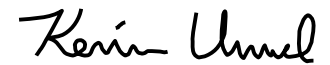
(3) For bibliographic and reference purposes this thesis should be referred to as:

Ummel, K. 2011. SEXPOT: A spatiotemporal linear programming model to simulate global deployment of renewable power technologies. Master of Science thesis, Central European University, Budapest.

Further information on the conditions under which disclosures and exploitation may take place is available from the Head of the Department of Environmental Sciences and Policy, Central European University.

## **AUTHOR'S DECLARATION**

No portion of the work referred to in this thesis has been submitted in support of an application for another degree or qualification of this or any other university or other institute of learning.

A handwritten signature in black ink that reads "Kevin Ummel". The script is cursive and fluid, with the first name and last name clearly distinguishable.

Kevin UMMEL

# CENTRAL EUROPEAN UNIVERSITY

**ABSTRACT OF THESIS** submitted by:

Kevin UMMEL

for the degree of Master of Science and entitled:

SEXPOT: A spatiotemporal linear programming model  
to simulate global deployment of renewable power technologies

Month and Year of submission: May, 2011.

---

This thesis introduces a computer model for simulating worldwide deployment of wind and solar power technologies at high spatial and temporal resolution. The Spatiotemporally-Explicit Power and Transmission (SEXPOT) model integrates global meteorological, geophysical, and socioeconomic data to identify cost-minimizing strategies for utilizing available renewable resources. SEXPOT is unique, because it allows for low-cost, large-scale analyses while providing local-scale results. Model output includes the preferred locations for wind and solar power technologies and transmission lines and shows how variable power sources can be integrated with conventional technologies to meet demand hour-by-hour. NASA climate model output is used to predict the performance of onshore and offshore wind turbines and utility-scale and rooftop solar photovoltaic (PV) panels, and a statistical model is developed to predict the distribution of electricity consumption across space and time. Linear programming techniques are then used to optimize the deployment of generating technologies. This paper describes the development of model components and associated input data and demonstrates functionality with an illustrative model run. Application to a variety of research questions is explored and areas for model improvement identified. SEXPOT is presently a working prototype that, it is hoped, will be improved over time.

**Keywords:** energy modeling, energy economics, greenhouse gas mitigation, low-carbon futures, electricity generation, geospatial analysis

---

## ACKNOWLEDGEMENTS

Helpful advice, comments, and data were provided by: Raymundo Aragão, Michael Bosilovich, Byron Byrne, Chris Elvidge, Reinhard Furrer, Paul Gardner, Paul Gilman, Jonathan Godt, Gregor Giebel, Kurt Hansen, Donna Heimiller, Trish Jackson, Daniel Kirschen, Kjell Konis, Ekaterina Kourzeneva, Xiao Li, Mark Mehos, Stephen Milborrow, Craig Mills, Myriam Neaimeh, Ksenia Petrichenko, Richard Sobonya, Byron Stafford, Jacob van Etten, and Michael Wagner.

Special thanks to Oscar Perpiñan and Robert Hijmans for their invaluable assistance applying the *solaR* and *raster* packages, respectively; to my advisors, Aleh Cherp and David Wheeler, for helpful comments; and to the European Commission and MESPOM Consortium for financial support.

My fiancé, Sarah, deserves sainthood for gracefully tolerating 5,000 miles of separation and, once together, graciously enduring more than a few SEXPOT dinner conversations. Thank you to my family and friends for their continued support and interest.

All remaining errors are mine and mine alone.

Comments and suggestions are most welcome: [SEXPOTmodel@gmail.com](mailto:SEXPOTmodel@gmail.com)

## TABLE OF CONTENTS

<b>Copyright and ownership.....</b>	<b>iii</b>
<b>Author's declaration.....</b>	<b>iv</b>
<b>Abstract.....</b>	<b>v</b>
<b>Acknowledgements .....</b>	<b>vi</b>
<b>List of tables and figures .....</b>	<b>viii</b>
<b>1. Introduction.....</b>	<b>1</b>
1.2 Aims and objectives.....	2
1.3 Model overview .....	3
1.4 Existing research.....	6
<b>2. Methods.....</b>	<b>9</b>
2.1 Wind, solar, and weather inputs.....	9
2.2 Identifying feasible generating sites .....	12
2.3 Modeling generating efficiency .....	14
2.4 Modeling electricity consumption .....	17
2.5 Specification of zones and nodes.....	20
2.6 Transmission line routing .....	22
2.7 Linear programming model .....	23
<b>3. Results of illustrative model run.....</b>	<b>28</b>
<b>4. Potential applications and improvements.....</b>	<b>34</b>
<b>5. Conclusion .....</b>	<b>37</b>
<b>References.....</b>	<b>39</b>
<b>Appendix A. Derivation of meteorological inputs.....</b>	<b>43</b>
A.1 Wind speed.....	43
A.2 Solar irradiance .....	43
A.3 Air density and relative humidity .....	44
<b>Appendix B. Technology performance models .....</b>	<b>46</b>
B.1 Wind turbine.....	46
B.2 Photovoltaic (PV) array.....	47

## LIST OF TABLES AND FIGURES

Figure 1: SEXPOT model schema.....	5
Figure 2: Annual solar power efficiency, feasible locales (2006) .....	15
Figure 3: Annual wind power efficiency, feasible locales (2006).....	15
Figure 4: Annual solar power efficiency over China, feasible locales (2006) .....	16
Figure 5: Annual wind power efficiency over Europe, feasible locales (2006) .....	16
Figure 6: Spatial distribution of electricity consumption (2006) .....	18
Figure 7: SEXPOT output showing renewable power sites in Asia .....	29
Figure 8: SEXPOT output showing transmission lines in northeast China and Mongolia.....	30
Figure 9: Summary of SEXPOT output for southeast U.S. ....	31
Figure 10: Disaggregated view of SEXPOT output for southeast U.S.....	32
Figure 11: Summary of SEXPOT output for northern India .....	33
Figure 12: Disaggregated view of SEXPOT output for northern India.....	33
 Table 1: Spatial layers used in terrain-screening algorithm .....	 12
Table 2: Assumed generating technology costs and CO <sub>2</sub> emission rates .....	25



## 1. INTRODUCTION

Over the next 25 years, global electricity use is likely to increase 75 to 90% (IEA 2010). The scale and speed of this growth has the potential to either exacerbate or mitigate global climate change, depending on the technologies deployed. Recognizing the potential for renewable energy to provide clean, low-cost electricity, more than 100 countries have enacted renewable energy promotion policies – often taking the form of a renewable electricity target (UNEP 2010). And should countries successfully implement voluntary pledges made under the Copenhagen Accord, renewable power generation is likely to triple by 2035 and attract investment of \$8 trillion (IEA 2010).

Still, prudent climate policy demands much more. Reaching a 450 ppm CO<sub>2</sub>-eq stabilization target will likely require power sector emissions to *decline* ~60% over the next 25 years – a challenge equivalent to replacing every fossil fuel power plant in operation today with a clean alternative. By comparison, voluntary pledges to date would lead to an emissions *increase* of ~15% (IEA 2010). While non-renewable, low-carbon technologies like nuclear power and carbon capture and sequestration (CCS) can play a role in achieving the necessary reductions, renewable power (especially wind and solar) remains central to mitigation strategies in many countries. Deploying these technologies quickly and cost-effectively is now a global priority.

The nature of renewable energy complicates this process. Unlike conventional thermal power technologies, which generate electricity where and when it is needed, renewable power requires that intermittent energy flows be harvested as they become available. And unlike hydroelectric dams, which allow potential energy to be stored and utilized as needed, renewable power must be consumed as it is generated.<sup>1</sup> Performance and cost is highly dependent on spatial and temporal characteristics. Understanding where, when, and how to use particular technologies, especially when considering large geographic areas, is a critical and complex task.

---

<sup>1</sup> There are many technical options for storing energy from renewable power generators (batteries, supercapacitors, flywheels, hydrogen, compressed air, pumped hydro, etc.), but their cost so far is prohibitive for large-scale applications (see Hadjipaschalis et al. 2009).

Addressing this challenge requires analyzing the interaction of renewable energy flows and electricity demand across space and time. The associated spatiotemporal complexity is too great for casual analysis; computer models are needed to “make sense” of the vast amounts of input data. Modeling makes it possible to identify particular locales, resources, and technologies that complement each other, revealing deployment strategies that maximize socioeconomic and environmental benefits. Making the best use of available resources – whether dollars of investment or megajoules of renewable energy – is critical to effective, forward-looking energy and climate policy.

## *1.2 AIMS AND OBJECTIVES*

This thesis introduces a computer model for simulating the worldwide deployment of wind and solar power technologies at high spatial and temporal resolution. The Spatiotemporally-Explicit Power and Transmission (SEXPOT) model, developed over the previous seven months, integrates a large amount of meteorological, geophysical, and socioeconomic data to identify cost-minimizing strategies for utilizing available resources. SEXPOT is unique among existing models, because it allows for large-scale analyses (including global simulations) while providing local-scale information. Model output includes the preferred locations of wind farms, solar power plants, and transmission lines and shows how variable power sources can be integrated with conventional technologies to meet demand hour-by-hour.

The aim of this thesis is *not* to perform a particular analysis but, rather, to describe the technical development of this tool and illustrate its functionality and potential applications. One objective is to show how SEXPOT’s model output can be used to increase understanding of two basic questions in the field in renewable energy:

- 1) *Where* are the best places to exploit renewable power resources?
- 2) *How* can these resources be spatially and temporally integrated into power systems?

Another objective is to identify a set of broader research questions that SEXPOT could help address in the future.

In Section 3, I use the results of a global simulation with SEXPOT to demonstrate how model outputs provide information relevant to the questions above. In Section 4, I “think big” about possible research applications and ways to improve the model. At present, the model is a functioning prototype that will, it is hoped, be developed over time.

### 1.3 MODEL OVERVIEW

The notion underpinning SEXPOT is simple: If we know where and when renewable energy is available and where and when electricity is needed, it should be possible to “match” these two phenomena in an optimal manner. The objective is to model the ways that renewable power technologies can be integrated into electricity systems and identify the particular arrangement that, for example, minimizes costs or CO<sub>2</sub> emissions. Most importantly, this approach is “spatiotemporally-explicit”; the model output reveals not only the optimal *quantity* of (for example) wind turbines but also *where* they could be located and *how* they could be used in conjunction with other technologies. In the case of SEXPOT, the goal is to do this at global scale.

A primary challenge in constructing such a model is a lack of input data. Information on the spatiotemporal distribution of wind speed, solar radiation, or electricity consumption, for example, is often fragmented, expensive, or simply unavailable (especially global data). Much of SEXPOT’s development has consisted of creating the necessary input data. NASA climate model output is used to predict the performance of wind turbines and solar photovoltaic (PV) modules for each point on Earth for every hour of the year. Nighttime satellite imagery is used to estimate the distribution of electricity consumption across space, and a statistical model is used to predict how it changes depending on the time of day and weather conditions.

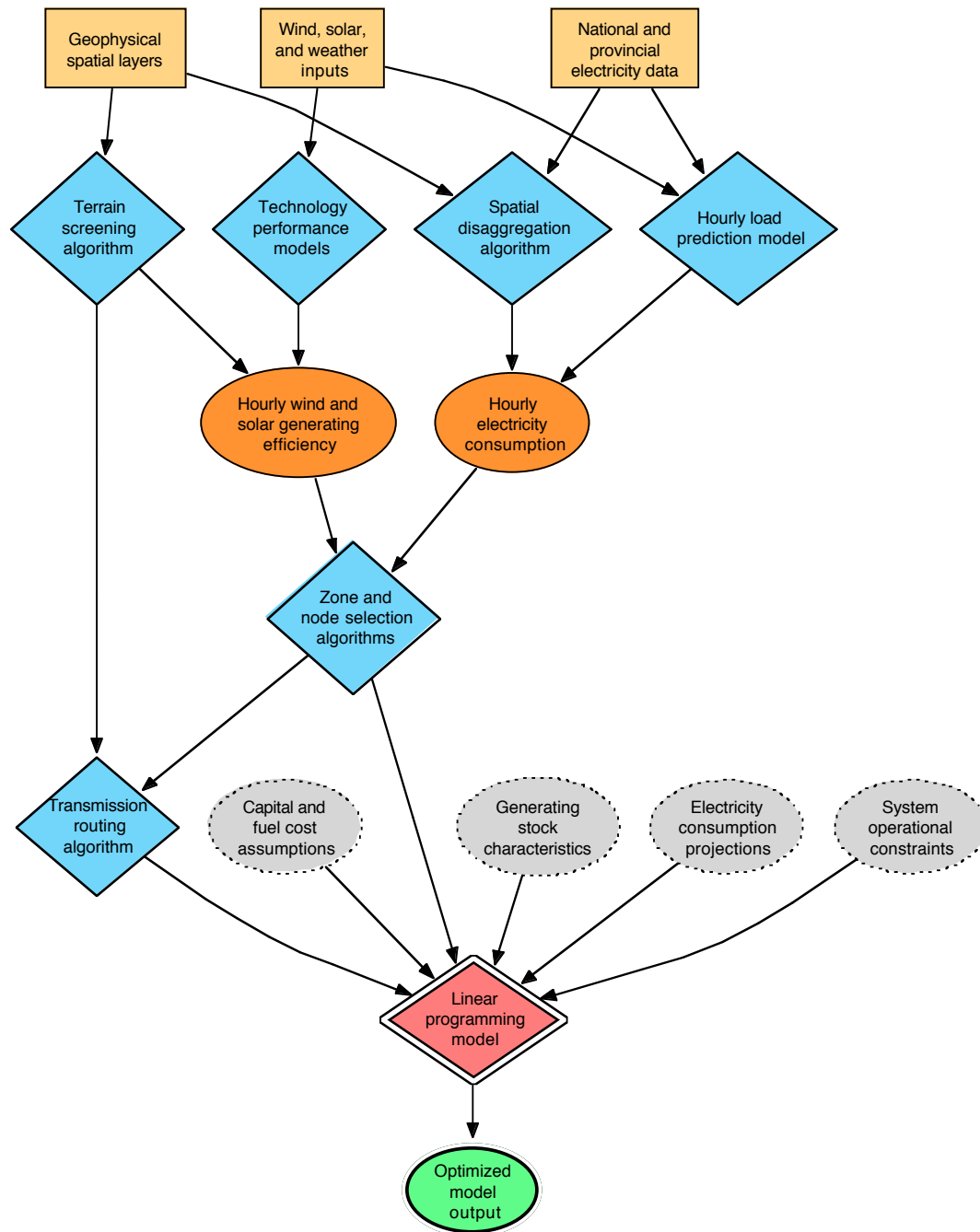
This data is fed into a mathematical model that mimics (roughly) the real-world operation of electricity markets. The model contains assumptions about the cost of different technologies and fuels, the efficiency of transmission lines, and the rate at which coal and gas plants emit CO<sub>2</sub>. It allows for the construction of onshore and offshore wind farms, utility-scale and rooftop PV, as

well as coal, gas, nuclear, and hydroelectric power. Remote generating sites are connected to demand centers by transmission lines that are placed using a spatial routing algorithm. The model is then asked to find the particular arrangement of technologies that succeeds in minimizing the overall cost while also meeting demand. Constraints forcing a limit on CO<sub>2</sub> emissions or a minimum penetration of renewable technologies can also be included. There is also the option to model future time periods that factor in expected growth in electricity consumption and retirement of ageing power plants.

Once the optimal solution is found, SEX POT turns the raw model output into graphical results. Visualizing results is important due to the quantity of output data; a moderate-size global model contains ~150,000 variables. Section 3 illustrates the kind of results provided by a typical model run. They show, for example, where each renewable power technology is optimally located; where transmissions lines are routed to connect generating sites to demand centers; and how different technologies can be combined to meet hourly demand over the course of a year.

Figure 1 provides a schematic overview of SEX POT's model components and data processing. A review of SEX POT's relation to existing energy model research is provided in the following section. Readers with interest in technical details will find descriptions of model components and input data in Section 2 and mathematical details in Appendices A and B. SEX POT is written in the open-source R Programming Language (R Development Core Team 2011) and makes particular use of the *raster* (Hijmans and van Etten 2011), *solar* (Perpinan 2011), *gdistance* (van Etten 2011), *earth* (Milborrow 2011), *rgdal* (Keitt et al. 2010), and *lpSolveAPI* (Konis 2011) packages; the latter two provide bindings to the open-source GDAL and lp\_solve libraries.

Figure 1: SEXPOT model schema



#### *1.4 EXISTING RESEARCH*

Energy modeling encompasses a vast body of research, reflecting the fact that different research questions require different models (see Connolly et al. 2010 for a review). Models incorporate the combination of technical complexity, sectoral breadth, geographic scope, and temporal detail required by their particular application; no single model can do it all. SEXPOT is concerned with understanding the spatial and temporal implications of renewable power technologies, which places it within a relatively recent and comparatively small body of research. The goal here is to briefly describe SEXPOT's feature set relative to general "energy-economy" models and highly-detailed power sector models.

A defining feature of SEXPOT is its explicit treatment of spatiotemporal data – meaning that it makes direct use of space- and time-specific information rather than using a reduced-dimension "summary" of that information. The latter approach is common among global or national energy-economy models, in part because such models include multiple sectors (not just electricity generation) and so must sacrifice spatiotemporal detail in the interest of sectoral breadth. These models are particularly valuable for modeling the consequences of new policies or fuel prices over time, generally operating at annual or multi-year time steps. Popular examples include the International Energy Agency's World Energy Model (WEM) and the U.S. Department of Energy's National Energy Modeling System (NEMS).

To capture the fact that renewable power is spatially-dependent, these models incorporate "supply curves" within a sub-model of the power sector. The curve is effectively an approximation of how the efficiency of a renewable technology is expected to decrease with penetration, reflecting the fact that prime locales are utilized first. The supply curves are intended to summarize a large amount of spatial (and sometimes temporal) information that is impractical to incorporate directly. This improves the realism of energy-economy models with respect to renewable power without unduly increasing model complexity.

An alternative approach is to treat spatial and temporal factors explicitly – modeling, for example, each hour of a year or season and representing each possible generating site

individually. This requires that the model be limited to the power sector (largely due to computational constraints), but it allows for high-resolution analysis of intermittency issues and project siting. While power engineers have long used mathematical optimization models to guide dispatch of conventional generating technologies (see Stott and Marinho 1979), the inclusion of renewable power is a relatively recent development. There is growing interest in using models to inform *integrated generation management* strategies (O'Connor 2010), whereby renewable resources are optimized across space and time to create an overall power supply that minimizes technical difficulties and cost. Recent modeling of California's renewable resources by Hart and Jacobson (2011) illustrates the usefulness of spatiotemporally-explicit models in identifying potential barriers to, and opportunities for, large-scale renewable power.

Prominent examples of this approach have been financed by the U.S. Department of Energy (DoE). Two large studies were carried out by a consortium of national labs, universities, and private firms to assess the cost and technical implications of integrating wind and solar power into U.S. electrical grids (EnerNex 2010; GE Energy 2010). These studies utilized a large amount of data regarding generator characteristics and transmission capacity and required expensive generation of high-resolution wind and solar resource datasets. The U.S. National Renewable Energy Laboratory also developed the Wind Deployment System (WinDS) and subsequent Regional Energy Deployment System (ReEDS), which has been used to assess the effect of proposed energy policies on U.S. renewable power penetration (DoE 2008; Short et al. 2009; Sullivan et al. 2009). In all cases, linear or mixed integer programming techniques are used to solve large-scale optimization problems.

Efforts such as those financed by the DoE are clearly the state-of-the-art approach to optimizing the use of resources within a region, but they depend upon the availability of detailed (and often proprietary) data, technical expertise, and large research teams (and accompanying budgets). SEXPOT takes the approach of these highly-detailed models and decreases the technical complexity while increasing the geographic scope. In this way, it provides a low-cost tool for global and continental-scale preliminary analysis, allowing the question of where, when, and how to use resources to be posed for much larger areas – and areas where the required input data for more complex models is lacking or difficult to obtain.

An example of a moderate-complexity, spatiotemporally-explicit model at global scale is that of Aboumahboub et al. (2010). They use moderate resolution solar radiation data (30 arc-minute; 3-hour intervals) and low resolution wind speed data (150 arc-minute; 6-hour intervals) to construct a global resource dataset. Gridded population estimates and representative load profiles are used to estimate hourly electricity demand across space. The data are integrated into a linear programming model designed to minimize the cost of meeting consumption in long-term energy scenarios. The approach is similar to that of a dissertation and subsequent work by Gregor Czisch (2006a; 2006b) that assessed the potential for an entirely renewables-based European power sector by utilizing resources in neighboring regions.

SEXPOT improves and expands upon these efforts by incorporating higher-resolution, hourly wind and solar resource and electricity consumption data, detailed site-selection and transmission-routing algorithms, and the built-in ability to visualize model output. It manages to combine a moderate level of technical complexity with global geographic coverage, while overcoming many of the data constraints facing large-scale analyses. In this respect, it fills an important gap in existing research: offering the potential for low-cost, high-resolution, preliminary assessment of renewable resource futures across large areas of the world.



## 2. METHODS

Sections 2.1 through 2.7 describe individual SEXPOT model components, techniques, and input datasets. Mathematical details can be found in Appendices A and B.

### 2.1 *WIND, SOLAR, AND WEATHER INPUTS*

The performance of renewable power technologies is largely determined by meteorological conditions. SEXPOT utilizes global, hourly information on resource magnitude (wind speed and surface irradiance) and important weather variables (temperature, humidity, etc.). Satellite data processing and numerical weather modeling are now standard techniques for generating consistent, large-scale renewable resource databases. Both use extensive information provided by satellite and the surface station records in conjunction with statistical and physical models to generate data at high spatial and temporal resolution.

SEXPOT's meteorological inputs are derived from output from NASA's Goddard Earth Observing System (GEOS-5) Model (Rienecker et al. 2008). As part of the Modern Era Retrospective Analysis for Research and Applications (MERRA) project, a global assimilation and reanalysis of the satellite and surface record was produced for the period 1979 to present. GEOS-5 provides the highest-resolution global reanalysis output currently available and is designed to provide initial and boundary conditions for operational weather forecasts and higher-resolution numerical weather models.

Although climate reanalyses are by no means ideal, they have a number of advantages for a model like SEXPOT. First, the assimilation and modeling process ensures that the output data contain no missing values across space and time. Second, the numerical models are able to provide “second-order” variables (like humidity) that are needed for renewable power modeling but difficult to obtain elsewhere. Finally, all output is spatially and temporally aligned, which makes subsequent data processing easier than attempting to integrate a series of regional

datasets.<sup>2</sup> Reflecting these advantages, reanalysis data has been used to model large-scale wind power potential in multiple studies (EEA 2009; Lu et al. 2009; McElroy et al. 2009).

GEOS-5 model output was downloaded from the online MERRA archive for every hour of 2006. While it is preferable to sample a longer period to account for inter-annual variation, a single year of data was used for reasons of convenience: 1) Complete 2006 data was required for spatiotemporal modeling of electricity consumption (Section 2.4) and 2) data storage and processing requirements for a longer period were prohibitive on the computer used to develop the SEXPOT prototype. Data were obtained at hourly time steps with a grid-cell resolution of  $0.67^\circ \times 0.5^\circ$  ( $\sim 67 \times 50$  km at the equator). The parameters included: ambient air temperature and specific humidity at 2 m above the displacement height; surface incident shortwave radiation flux and albedo; and zonal (eastward) and meridional (northward) wind speed at 2 m, 10 m, and 50 m above the displacement height, along with monthly mean displacement height and a surface elevation layer. All data were bilinearly resampled to a node-registered grid for compatibility with other spatial datasets.

Although the complete year 2006 data includes 8,760 observations (24 hours x 365 days) for each cell-variable, this is compressed to reduce the computation time throughout SEXPOT's processing chain. For each variable, a mean 24-hour period is calculated for each month of the year, effectively reducing the number of hours under consideration to 288 (24 hours x 12 months). The algorithms and submodels described in following sections utilize this 288-hour dataset. The final SEXPOT optimization routine (Section 2.7) can make use of 96- or 32-hour summaries derived from the 288-hour data.

The raw GEOS-5 data are transformed into the specific variables required for modeling wind and solar power technologies. For wind turbines, the primary input is wind speed at hub height, which is assumed to be 80 m onshore and 120 m offshore. For each grid cell and hour, GEOS-5

---

<sup>2</sup> A private company recently introduced worldwide, high-resolution wind speed and solar irradiance datasets derived from satellite data and numerical weather modeling. The cost, however, is prohibitive for global-scale analysis. GEOS-5 is the next best option and is entirely free to use. For the purposes of developing a SEXPOT prototype, the moderate resolution GEOS-5 output provides a good balance between spatial detail and computation time. That said, SEXPOT is able to utilize high(er)-resolution data if available.

wind speed at 2, 10 and 50 m above the displacement height is used to estimate the wind speed at 80 and 120 m above the surface. This is done by fitting a power law function to the GEOS-5 observations and extrapolating (or, in some cases, interpolating) to the necessary hub heights, making adjustments for cell and time-specific vegetation height.<sup>3</sup> The power law is a common technique for modeling the observed relationship between wind speed and height within the atmospheric surface layer (Elliott et al. 1986; Archer and Jacobsen 2005).

For solar power, the critical variable is effective solar irradiance on a receiver (e.g. a PV module). This quantity is a function of surface irradiance, sun position, and receiver characteristics. GEOS-5 surface shortwave irradiance (i.e. global horizontal irradiance) is processed using the *solaR* package. Decomposition of global irradiance into diffuse and direct components makes use of a statistical technique developed by Ridley et al. (2010). Hourly effective irradiance is calculated for both fixed-tilt rooftop PV and single-axis tracking PV arrays; indirect (reflected) radiation is taken into account using modeled surface albedo from GEOS-5. The optimal tilt angle and array row spacing are internally calculated for rooftop and utility installations, respectively.

While wind speed and solar irradiance are the primary variables, temperature and humidity have secondary effects on technology performance. They are also critical to modeling the response of electricity demand to weather conditions (Section 2.4). Ambient temperature is provided directly by GEOS-5. Relative humidity is derived from GEOS-5 specific humidity by way of an approximation of air density using ambient temperature and elevation. Details of calculations to derive input weather variables can be found in Appendix A.

---

<sup>3</sup> The displacement height is the *effective* surface height, typically about two-thirds the mean height of obstacles. Wind speed is zero at displacement height of zero. For heavily forested areas, the GEOS-5 50 m (above displacement height) wind speed may exceed 80 m above the surface. In these cases, the power law function effectively interpolates the 80 m wind speed.

## 2.2 IDENTIFYING FEASIBLE GENERATING SITES

A high-resolution terrain-screening algorithm is used to identify suitable sites for each renewable generating technology. Requirements differ among technologies, reflecting engineering needs and social preferences.

The primary input is a high-resolution dataset developed by the European Space Agency and the Université catholique de Louvain for year 2009, capable of resolving land cover at  $\sim 300 \times 300$  m resolution. Further screens are provided by secondary datasets, typically at  $\sim 1 \times 1$  km resolution. Table 1 lists the 11 geophysical data layers used within the terrain-screening algorithm.

Table 1: Spatial layers used in terrain-screening algorithm

<u>Geophysical layer</u>	<u>Description</u>	<u>Resolution</u>
Land cover	Globcover (v2.3) classification of global land cover as observed during year 2009 by the MERIS instrument onboard the ESA's Envisat satellite (Bontemps et al. 2010).	10'' (~300m)
Terrain slope	Mean slope derived from 90-meter SRTM elevation (Verdin et al. 2007).	30'' (~1km)
Population density	Derived from LandScan™ population count layer produced by ORNL (2008).	30'' (~1km)
Geomorphology	Hazardous landforms (glaciers, rock outcrops, salt flats, and sand dunes) from the Harmonized World Soil Database (FAO et al. 2009).	30'' (~1km)
Elevation and bathymetry	ETOPO1 global relief model (relative to ice surface) developed by NOAA (Amante and Eakins 2009).	60'' (~2km)
Lakes and wetlands	Inland water classification from the Global Lakes and Wetland Database (Lehner and Döll 2004).	30'' (~1km)
Lake depth	Mean depth of inland water bodies (Kourzeneva 2009; 2010).	30'' (~1km)
Protected areas	Derived from global vector dataset of the World Database on Protected Areas (IUCN and UNEP 2010).	30'' (~1km)
Rooftop area	Derived from the global urban characteristics dataset of Jackson et al. (2010), using availability factors from Izquierdo et al. (2008).	30'' (~1km)
Travel time (onshore)	Travel time over land surface to the nearest city of at least 50,000 people (Nelson 2008).	30'' (~1km)
Travel time (offshore)	Derived by author for ocean cells using the onshore travel time surface in conjunction with a distance sampling and interpolation algorithm.	5' (~10km)

For all technologies, geomorphologic hazards (sand dunes, glaciers, rock outcrops, and salt flats), protected areas of any kind (terrestrial or marine), and wetland/estuarine environments are excluded. Excessively remote locales are excluded using the travel time surface of Nelson (2008), which integrates information from multiple underlying datasets. Land-based projects require that a city of at least 50,000 people could (potentially) be reached within three hours drive on paved roads. Offshore wind projects are allowed up to 100 km from a coastal locale that is already within two hour's travel of an urban center.<sup>4</sup>

The following describes technology-specific screening criteria:

- Onshore wind: All land cells feasible except those characterized by artificial surfaces, population density greater than 150 persons per km<sup>2</sup>, or mean slope greater than 20%. Forested areas are assigned 50% availability, reflecting clearing and access restrictions.
- Offshore wind: All ocean and lake cells feasible where water depth does not exceed 200 m, subject to travel time constraint. Reservoirs are excluded.
- Utility-scale PV: Restricted to cells characterized by bare ground, shrubland, and sparse or herbaceous vegetation, population density less than 150 persons per km<sup>2</sup>, and mean slope less than 3%.
- Rooftop PV: Restricted to settled areas exhibiting electricity consumption. Usable roof area is a function of building characteristics (Jackson et al. 2010) and availability factors (Izquierdo et al. 2008).

Total feasible land area is aggregated from the high-resolution land cover layer after making necessary exclusions. A spatial layer is then derived at 5-minute resolution (~10 x 10 km), indicating the land area available to each technology within a given grid cell.

---

<sup>4</sup> Assuming construction of project-specific access roads cannot exceed 50 km and that travel speed is 60 km per hour on major roads and 36 minutes per km on unpaved, flat terrain, the maximum allowable onshore travel time in the Nelson surface is:  $(3-50/60)*60 + 50*36 = 1,930$  minutes. In the offshore case, an assumed over-water travel speed of 20 km per hour gives a maximum allowable travel time of:  $2*60 + (100/20)*60 = 420$  minutes.

### 2.3 MODELING GENERATING EFFICIENCY

The generating efficiency of each technology is modeled hour-by-hour for feasible areas. The performance models incorporate data on the magnitude of the primary renewable resource (i.e. wind or sunlight) as well as secondary weather variables. For example, wind turbine efficiency depends not only on wind speed but also air density, which is a function of air temperature and elevation. Similarly, photovoltaic module performance is determined by incident radiation and cell temperature, the latter a function of air temperature, wind speed, and panel mounting (i.e. roof- or rack-mounted). SEXPOT's efficiency models incorporate all of these factors to create realistic estimates of hourly generating potential.

The wind turbine performance model is based on a modified logistic function fit to a dataset of power curves for commercial turbines. The turbine model also incorporates an hourly air density correction and assumes constant mechanical and electrical losses of 10%. The air density correction is important for particular regions; turbines operating in the thin air of the Tibetan Plateau, for example, exhibit efficiency ~30% lower than expected at sea level for the same wind speed. The PV performance model uses the simple efficiency model of Menicucci (1986) in conjunction with the cell temperature and inverter efficiency equations of King (2007) and default derate losses from NREL's System Advisor Model (Gilman et al. 2008). The reference module is a First Solar FS-272 thin-film (CdS/CdTe semiconductor) module; the mounting technique is allowed to vary between rooftop and utility-scale PV applications. Details are provided in Appendix B.

Combining the results of the feasible site analysis in Section 2.2 with the generating efficiency models allows expected performance across space and time to be plotted. Figures 2 and 3 report global mean generating efficiency of solar and wind power technologies, respectively, over the course of 2006 for all feasible locales. Figures 4 and 5 provide geographic insets for China (solar) and Europe (wind), respectively. Movies showing the hourly progression of solar and wind generating efficiency over the course of 2006 can be viewed at:

[http://dl.dropbox.com/u/14314000/ThesisMedia/SolarEfficiency\\_2006\\_Global.mov](http://dl.dropbox.com/u/14314000/ThesisMedia/SolarEfficiency_2006_Global.mov)

[http://dl.dropbox.com/u/14314000/ThesisMedia/WindEfficiency\\_2006\\_Global.mov](http://dl.dropbox.com/u/14314000/ThesisMedia/WindEfficiency_2006_Global.mov)

Figure 2: Annual solar power efficiency, feasible locales (2006) <sup>5</sup>

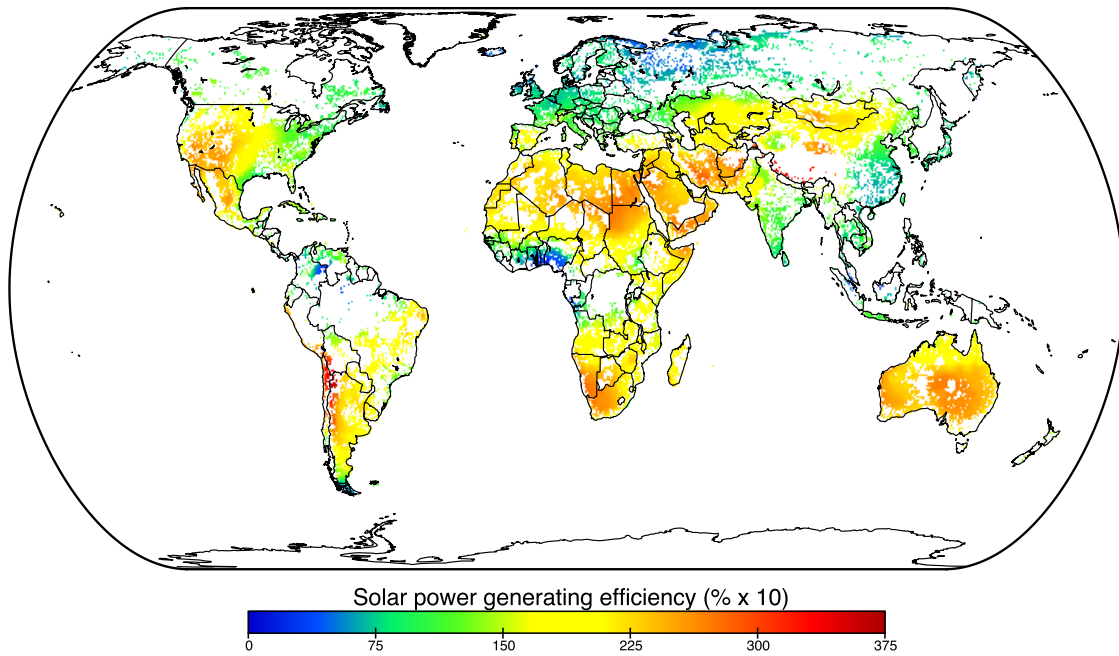
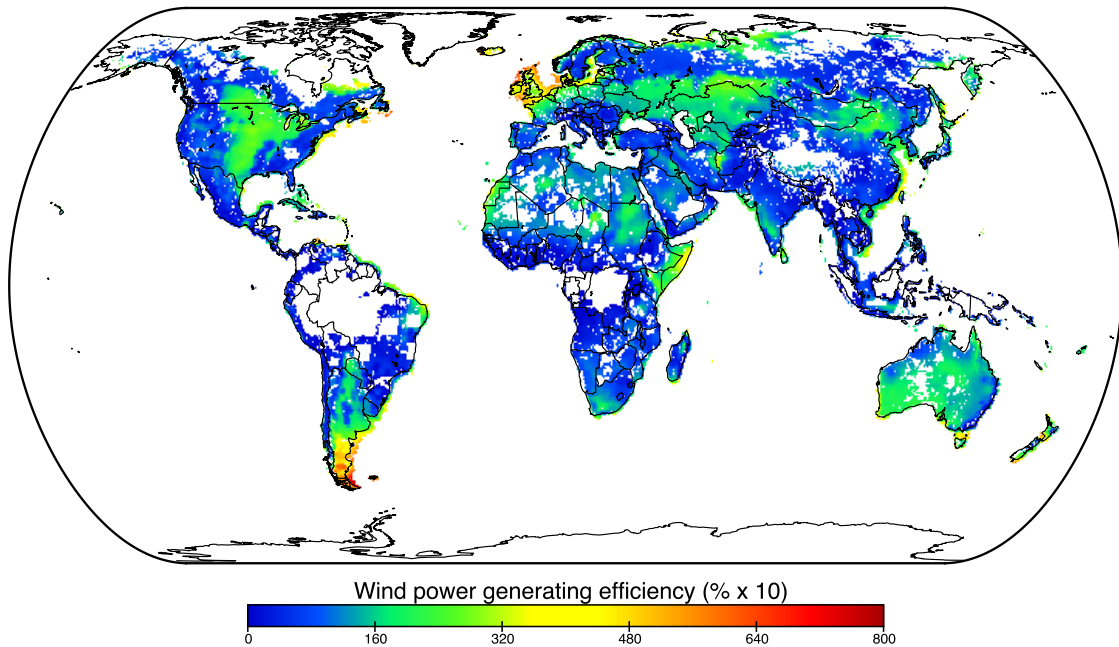


Figure 3: Annual wind power efficiency, feasible locales (2006)



<sup>5</sup> The data in Figures 2 through 5 (and associated movies) are generated within SEX POT, using techniques described in Sections 2.1-2.3 and Appendices A and B. The units are percentage efficiency (i.e. capacity factor) multiplied by 10; for example, a value of 300 indicates a locale that is able, on average, to generate output equal to 30% of installed capacity. Maps and animations are produced with NASA's Panoply software.

Figure 4: Annual solar power efficiency over China, feasible locales (2006)

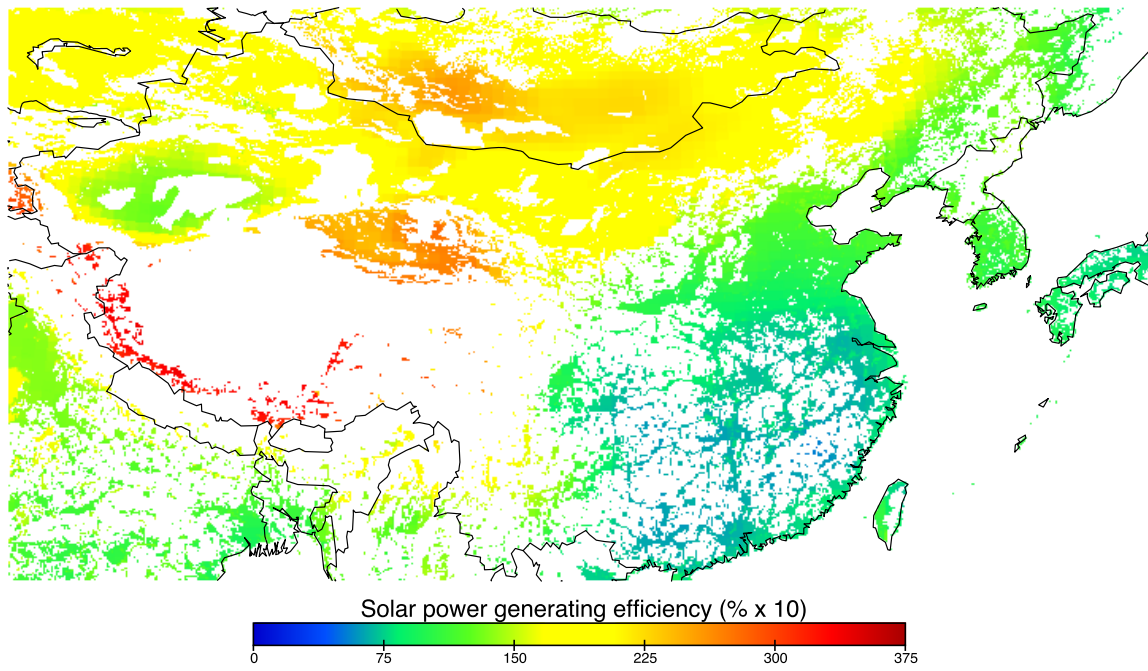
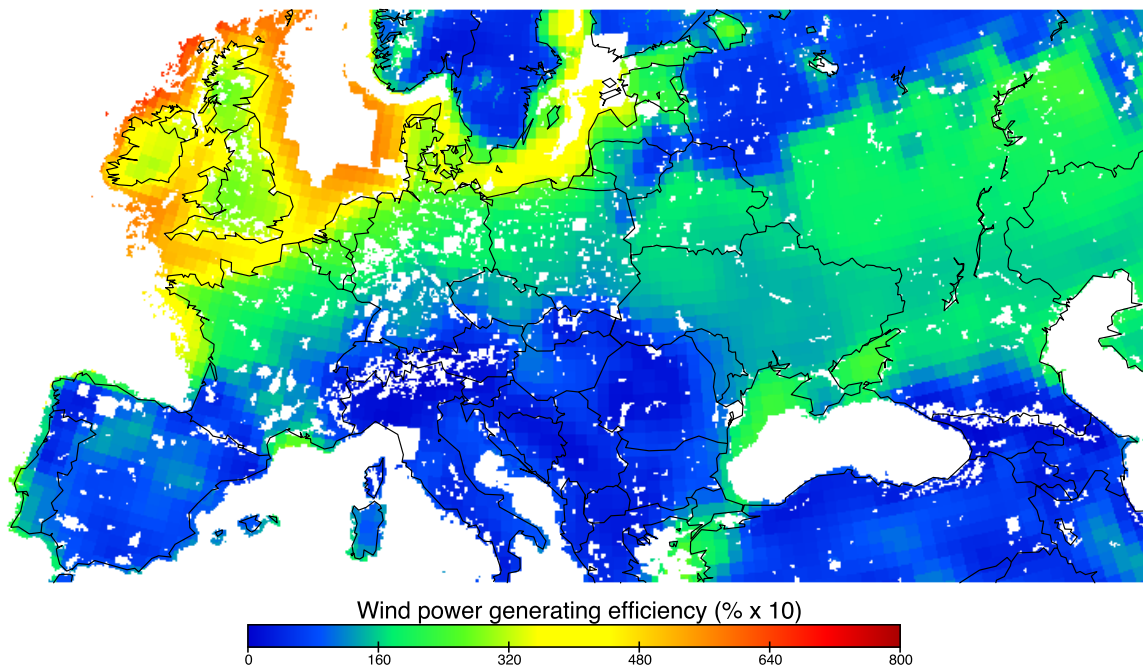


Figure 5: Annual wind power efficiency over Europe, feasible locales (2006)



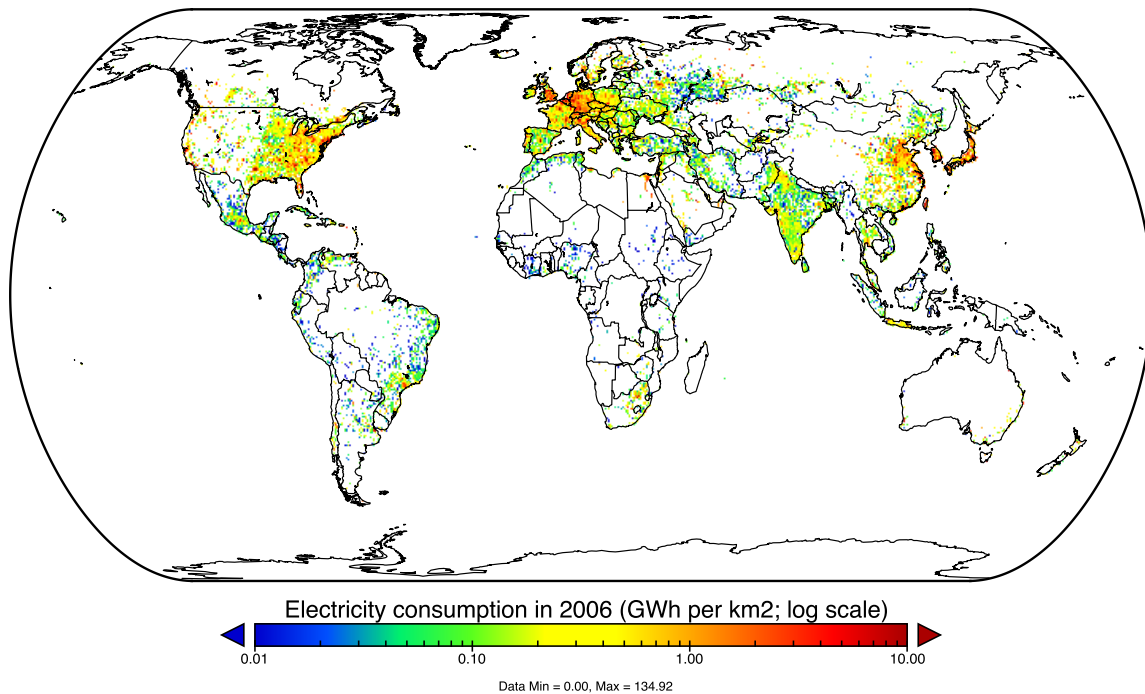


## 2.4 MODELING ELECTRICITY CONSUMPTION

Deriving estimates of hourly electricity consumption at global scale is a two-part process. First, the spatial distribution of annual consumption is estimated, using the intensity of stable nighttime lights to allocate national and sub-national electricity consumption. The nighttime lights imagery consists of a 1 km resolution calibrated product for 2006 that accounts for light saturation in urban areas (NOAA 2009). Previous studies have shown such data to be good predictors of electricity consumption across space (Amaral et al. 2005; Chand et al. 2009; Letu et al. 2009; Ummel 2010a).

Reported 2006 electricity consumption for more than 200 countries was obtained from the U.S. Energy Information Administration. For the U.S., Canada, Brazil, Russia, China, India, and Australia, consumption (or, in some cases, generation) totals were obtained for individual states/provinces from national statistical offices. The distribution of national or (when available) sub-national consumption across associated grid cells is assumed to be proportional to the distribution of nighttime light intensity. The final product consists of a 5-minute resolution dataset giving the estimated annual consumption per grid cell (Figure 6).

Figure 6: Spatial distribution of electricity consumption (2006)<sup>6</sup>



In order to estimate hourly consumption, reported load was obtained for each hour of 2006 for 26 electricity markets in Europe and Australia (ENTSO-E and AEMO public databases). The markets coincide with country boundaries in Europe and state boundaries in Australia. Using the annual consumption layer in conjunction with hourly GEOS-5 model output, consumption-weighted mean meteorological variables were calculated for each market and hour of the year. The load and GEOS-5 data were then temporally aligned, taking into account time zone and daylight savings adjustments.

For each market, mean and maximum observed load as well as mean ambient temperature, relative humidity, surface irradiance, and wind speed were calculated for 288 time periods (i.e. a 24 hour period for each of 12 months). Since the markets differ in climate regime and size, the raw variables were standardized to allow comparison. Mean and maximum hourly load were scaled relative to the annual mean load; the weather variables were converted to annual z-scores (i.e. the number of standard deviations from the annual mean value). Lagged effects were

<sup>6</sup> Data generated within SEXPOT using techniques described in Section 2.4.

captured by including the mean z-score over the previous three hours for each weather variable. The resulting dataset provides coherent load and weather information for about 7,500 observations (288 observations for each of 26 markets).

Weather conditions and temporal characteristics (i.e. time of day, day of week, etc.) are regularly used to predict electricity consumption for a range of applications (Feinberg and Genethliou 2005; Hahn et al. 2009). Building a predictive model, however, is complicated by the potential for non-linear relationships between variables. For example, ambient temperature may exhibit a piece-wise linear relationship with load, with a “knot” point at the temperature where consumers switch between cooling and heating appliances. Depending on the time of day or season, the slope of the linear segments about the knot may differ – as could the number of knots. These factors complicate *a priori* selection of an appropriate functional form.

To address this, a multivariate adaptive regression spline (MARS) approach is used to model the relationship between meteorological and temporal variables (the regressors) and load (the dependent variable). MARS is implemented via the *earth* package, using the approach of Friedman (1991). In short, MARS allows for piece-wise “hinge” functions to be adaptively fit to training data – no functional form must be specified beforehand. After adding hinge terms until the model’s residual error is stable, a “backward pass” uses a generalized cross validation criterion to discard terms in an attempt to produce a parsimonious model.

Two MARS models were fitted to the dataset; one to predict mean hourly load and one to predict peak (maximum) load. Both are a function of (standardized) mean weather variables and the time of day, with potential interaction between pairs of variables (i.e. a two-degree model). Given the complexity of the resulting functional forms, the results are only summarized here. Predictive power is indicated by a  $GR^2$  value, which is analogous to  $R^2$  in standard linear regression but penalizes overfit models. The models capture 64-69% of the variation in load using only the time of day and weather conditions as predictors. Inclusion of market fixed-effects increases  $GR^2$  to above 0.80, suggesting that future inclusion of country-specific variables (for example, the relative contribution of electricity to overall energy use) could improve predictive power. In both models, the time of day and temperature are the most important predictors. For the peak load

model, lagged temperature matters more than instantaneous temperature – correctly capturing the “build up” phenomenon characteristic of peak demand periods.

The MARS model is used to temporally disaggregate the global, annual consumption layer, resulting in estimated mean and peak load for each of 288 hours for every grid cell. A movie showing the hourly progression of electricity consumption over the course of 2006 can be viewed at:

[http://dl.dropbox.com/u/14314000/ThesisMedia/ElectricityConsumption\\_2006\\_Global.mov](http://dl.dropbox.com/u/14314000/ThesisMedia/ElectricityConsumption_2006_Global.mov)

## *2.5 SPECIFICATION OF ZONES AND NODES*

Ideally, all of the spatiotemporal data developed in Sections 2.3 and 2.4 could be analyzed to determine optimal deployment patterns. In practice, the computational demands are prohibitive, and it is necessary to “compress” the data into a smaller number of observations. This is unproblematic so long as the chosen subset of data captures all (or nearly all) of the critical information. SEX POT uses heuristic algorithms to select the most useful pieces of input data, allowing the scale of the optimization problem to be reduced. The algorithms select a subset of potential renewable energy sites and consumption centers that are likely to give results similar to that of an unconstrained model.

SEX POT models the movement of electricity between “nodes” (points in space), each of which is embedded in a “zone” (an area in space). Electricity flows from production zones/nodes to consumption zones/nodes. For example, the ERCOT electric grid in Texas is a consumption zone; SEX POT’s treatment of zones is analogous to that of “balancing areas” in power system engineering. Within the ERCOT consumption zone, there are multiple potential nodes – places at which electricity transmitted from outside ERCOT can be “hooked up” to the distribution grid.

While consumption zones correspond to the physical boundaries of power systems (typically national grids), production zones are circular areas incorporating all (potential) renewable power generating sites within a given radius. Each production zone has a single node – the point from which electricity is transmitted to consumption nodes. By controlling the size of zones and

number of nodes, the complexity of the optimization problem can be scaled up or down depending on analytical objectives and computational power.

Selection of consumption nodes begins by identifying cells on the perimeter of electrified areas where transmission infrastructure is feasible (i.e. suitable population density, terrain, etc.). The algorithm then proceeds zone-by-zone, taking a sample of feasible nodes and identifying those that are best situated with respect to electricity consumption. Nodes are selected sequentially, subject to the constraint that each be separated by at least 500 km. The result is a rank ordering of possible consumption nodes worldwide, from which a given number can be selected depending upon the desired model complexity.

Using the data developed in Section 2.3, a global set of potential renewable power production sites is created, assuming circular zones with radii of about 30 km. SEXPOT prioritizes sites that exhibit potential to provide low-cost GHG abatement. The approximate cost of GHG abatement ( $A$ ) for a given site and technology is proportional to a function incorporating capital costs ( $C$ ), generating efficiency ( $E$ ), the distance between production and consumption ( $d$ ; km), and the GHG intensity of existing electricity supply ( $G$ ):

$$A \approx \frac{\text{Production cost} + \text{Transmission cost}}{\text{Emissions averted}} \propto \frac{\frac{C}{E} \left( 1 + \frac{d}{10^4} \right)}{G}$$

where the  $d$ -dependent transmission cost component is assumed to increase production costs by ~1% for every 100 km (Ummel 2010b). This relationship is used to derive a heuristic “fitness” statistic for each production site that is used to rank order sites based on their ability to contribute to global GHG abatement. For each potential cluster node  $n$  and technology  $T$ , the fitness statistic ( $F$ ) is given by:

$$F_{n,T} = \frac{G_n}{\frac{C_T}{E_{n,T}} \left( 1 + \frac{d_n}{10^4} \right)}$$

where  $E_{n,T}$  is the capacity-weighted mean annual generating efficiency of technology  $T$  within cluster  $n$ ;  $d_n$  is the consumption-weighted mean distance to demand (km) within search radius  $r_c$  (assumed to be 2,000 km); and  $G_n$  is the consumption-weighted mean GHG intensity of existing generation within search radius  $r_c$ .  $C_T$  is the technology-specific capital cost (assumed values given in Section 2.7).

Note that the  $F$  statistic alone is not sufficient to select a subset of production zones, as it does not consider constraints imposed by electricity demand. For example, some sites may exhibit a low cost of abatement (as evidenced by a high  $F$  statistic), but there may not be much nearby demand. Or a large number of ideal production sites will be close to one another, but only a handful are required to meet nearby demand. A preferred set of clusters will provide enough geographic diversity to allow the model to be solved for a variety of scenarios, some of which may call for steep emissions reductions requiring that the clusters be sufficiently “spread out”.

An algorithm uses the  $F$  statistic to guide the selection of a diverse set of production zones, moving sequentially and “removing” demand as it is met by supply. In this way, the algorithm forces selection of a more geographically varied set of sites. “Tuning” parameters within the algorithm give the user some control over the results.

## 2.6 TRANSMISSION LINE ROUTING

Once consumption and production nodes are identified, a “least-cost path” algorithm is employed to 1) determine which pairs (“dyads”) of consumption and production points are feasible – that is, it is possible to construct a transmission line between them; and 2) if feasible, calculate the total length of the transmission line. The process employs Dijkstra’s graph search algorithm (Dijkstra 1959) as implemented via the *gdistance* package. The algorithm identifies the geographic path that minimizes the cost of crossing a surface.

SEXPOT’s transmission cost surface consists of a 5-minute resolution (~10 x 10 km) raster layer, where each cell contains an estimate of the topographic distance of crossing the cell (i.e. accounting for average terrain slope). The layer also excludes terrain unsuitable for line

construction (geomorphologic hazards, extreme slope, protected or heavily-populated areas, etc.). Underwater transmission via submarine cable is allowed across cells where depth does not exceed 2,000 m. A 5-minute layer is used to ensure reasonable computation time for a global model run. For analyses at smaller geographic scale, however, the transmission cost surface is capable of using grid cells as small as  $\sim 1 \times 1$  km.

A dyad is deemed infeasible if a path cannot be found between the points (e.g. a large sand dune surrounds one of the points) or the transmission line length exceeds 2,000 km. A given production node may have feasible routes to multiple consumption nodes within a zone, but only the shortest path is retained. The resulting matrix gives the shortest feasible transmission distance required to link any production zone to any other consumption zone (subject to the 2,000 km limit). The LP model (Section 2.7) uses this information to calculate transmissions costs and power losses.

## 2.7 *LINEAR PROGRAMMING MODEL*

Linear programming is an optimization technique in which a linear “objective function” is minimized or maximized subject to a set of linear constraints. Provided the phenomena of interest can be described with linear relationships, the comparatively short solve time of most “LP” models makes them ideal for large-scale optimization tasks. SEXPOT creates a LP model in which the objective function specifies the total cost of providing electricity; the model is then solved to find the variable values that minimize the cost function subject to constraints. This section provides a brief (non-mathematical) description of the optimization model.

In general, the cost of providing electricity consists of three components: 1) capital costs associated with building facilities; 2) variable costs incurred with each unit of electricity produced (e.g. fuel costs); and 3) the cost of transmitting and distributing electricity to consumers. SEXPOT’s LP cost function includes all three components. Variable costs are determined by the amount of electricity generated and the technologies used to do so; capital costs are incurred when new facilities are built; and transmission costs are the result of lines and substations needed to connect remote generating sites to demand centers.

The cost function can include thousands of variables, each of which specifies the amount of electricity to be generated by a given technology in a given place in a given hour and consumed in a given consumption zone. Other variables track the construction of new capacity of a given technology in a given place. Other track the construction of new transmission lines.

The total cost of meeting demand depends not only on the amount and type of power generated but also technology-specific cost assumptions. Assumed capital and operation and maintenance (O&M) costs for all technologies as well as CO<sub>2</sub> emission rates for coal and gas power come from the U.S. Annual Energy Outlook 2011 (EIA 2010). Fuel costs are estimated using current coal and gas prices. These values are summarized in Table 2 (see footnotes for fuel cost details).

To make the cost components consistent with the LP specification, reported fixed O&M is converted to a variable cost (\$/MWh) using an assumed annual capacity factor. Combined with the variable O&M component, this constitutes the total variable cost of generation and specifies the cost of each MWh generated within the LP. Facility capital costs are annualized, assuming a real discount rate of 7% and project lifetime of 20 and 40 years for renewable and conventional technologies (including transmission), respectively. Transmission costs are set to \$200 per MW-km based on published cost figures for HVAC and HVDC technologies (Ummel 2010b). Operating costs of transmission are minor and not included; lines losses are set to 1% per 100 km.



Table 2: Assumed generating technology costs and CO<sub>2</sub> emission rates

Technology	Capital cost (\$/W)	Fixed O&M (\$/MWh) <sup>7</sup>	Variable O&M (\$/MWh)	Fuel cost (\$/MWh)	Total variable cost (\$/MWh)	CO <sub>2</sub> emission rate (kg/MWh)
Onshore wind	2.44	10.7	0	0	10.7	0
Offshore wind	5.98	20.3	0	0	20.3	0
Utility PV	4.76	7.63	0	0	7.63	0
Rooftop PV	6.05	11.9	0	0	11.9	0
Coal	3.17	4.83	4.25	34.8 <sup>8</sup>	43.9	822
Gas CC	0.98	1.93	3.43	58.4 <sup>9</sup>	63.8	377
Nuclear	5.34	11.9	2.04	7.28 <sup>10</sup>	21.2	0
Hydroelectric	3.08	3.06	0	0	3.06	0

The LP's linear constraints ensure that the values assigned to the cost function variables follow certain rules. For example, one requirement is that electricity demand be satisfied (a power system that doesn't produce any power is certainly cheap, but it's not particularly useful, either). Other constraints ensure that wind and solar power do not exceed the amount of available land in a given production zone. By imposing additional constraints, one can force the model to achieve certain outcomes. For example, it is possible to force total CO<sub>2</sub> emissions to remain below a certain level, or force total output from wind and solar facilities to achieve a minimum percentage of overall power generation.

SEXPOT allows the LP model to utilize coal, gas, nuclear, and hydroelectric power – in addition to wind and solar power – to meet demand in a cost-minimizing fashion. For simplicity, the model assumes there is no existing wind and solar capacity in operation, but it does incorporate estimates of available conventional generating capacity. Using data from a proprietary database on power plant characteristics along with the Carbon Monitoring for Action (CARMA) public

<sup>7</sup> Fixed cost in \$/MW converted to \$/MWh assuming annual capacity factor of 85% for coal, gas, and nuclear; 50% for hydroelectric; 25% for solar; and 30% for wind.

<sup>8</sup> Assumes steam coal price of \$3.96 per MMBtu (average 2010 Newcastle f.o.b. price of \$98.98 per metric ton at 25,000 Btu per kg; World Bank commodity price data) and nominal heat rate of 8,800 Btu/kWh.

<sup>9</sup> Assumes natural gas price of \$8.29 per MMBtu (average 2010 European NG price; World Bank commodity price data) and nominal heat rate of 7,050 Btu/kWh.

<sup>10</sup> Assumes fuel cost of \$0.70 per MMBtu and nominal heat rate of 10,400 Btu/kWh (Deutch et al. 2009).

power plant database (Wheeler and Ummel 2008), it is possible to estimate the amount of coal, gas, nuclear, and hydroelectric capacity in each consumption zone. It is also possible to estimate the extent which these capacities will decline over time as plants reach the end of their expected operating lifetime and are forced to retire. Since it is comparatively cheap to make use of capacity already in place, the age structure and associated rate at which coal and gas plants retire in different regions is an important factor in determining the cost-competitiveness of wind and solar power across space and time.

SEXPOT includes a comparatively limited set of constraints on conventional generating technologies. Highly-detailed models like those recognized in Section 1.4 contain many more constraints on the operation of individual plant types. For example, SEXPOT does not (yet) specify the “ramp” or “turndown” rates of coal and nuclear power plants. In reality, these thermal plants are not able to turn “off” and “on” or quickly accelerate output as presently allowed. In addition, there are no site-specific limitations to the price or availability of natural gas. In reality, gas faces geographic barriers that alter costs and feasibility depending on the region.

Hydroelectricity presents a particular modeling challenge, because it is only partly dispatchable and the operating rules are unknown. In reality, the generating potential at any given time is constrained by current water level and expected inflows and outflows (which will vary seasonally). SEXPOT employs a simple constraint that allows hydroelectric power output within a given zone to freely ramp output up and down as long as the annual capacity factor does not exceed the value estimated for 2007 using data from CARMA. Because the variable cost of hydroelectricity is so low, this constraint is needed to prevent hydroelectricity from unrealistically dominating supply. SEXPOT presently places no limitations on new nuclear capacity, *except* to restrict capacity expansions to countries already using nuclear power.

An important cost component of power systems attempting to integrate renewable power is the additional cost required to maintain system stability. If renewable power supply is highly variable, the system may require additional gas plants to provide sufficient backup in cases where demand is high but wind power output low. SEXPOT (very roughly) accounts for this by

explicitly modeling the maximum (peak) expected demand for each consumption zone. The LP model is thereby forced to provide sufficient backup capacity to meet peak demand *under average generating conditions*. This is still an underestimate of the required reserve, however, since the reserve capacity must be large enough to meet peak demand under (nearly) *worst-case* generating conditions (i.e. unusually low wind speed or radiation levels, unplanned plant outages, etc.). There are ways to better represent this in the LP, but at present SEXPOT utilizes only a very simple constraint.

The LP model can be run using either 96 model hours (a 24-hour period for each of four seasons) or 32 model hours (eight 3-hour periods for each of four seasons). Overall LP model size and computation time are highly dependent on the temporal resolution. At present, SEXPOT is constructed to optimize the LP model for a single year at a time. There is the ability, however, to model future time periods by adjusting the electricity consumption values to reflect future growth. SEXPOT uses the EIA's 2010 International Energy Outlook country and regional electricity projects to predict electricity consumption up to 2035.

### 3. RESULTS OF ILLUSTRATIVE MODEL RUN

A single model run at global scale is used to illustrate SEXPOT's basic functionality. The simulation included 70 consumption zones accounting for ~90% of global electricity consumption, 400 potential renewable power sites, and 96 simulation hours (a 24-hour period for each of four seasons). The simulation is for a single, future year (2035) and corresponds to the IEA World Energy Outlook's "450 Scenario" in which power sector CO<sub>2</sub> emissions total ~5,000 Mt and wind and solar power provide 20% of global generation in 2035 (IEA 2010).<sup>11</sup> Capital, O&M, and fuel cost assumptions are unadjusted from the present. Electricity demand in each consumption zone is projected forward to 2035. The resulting LP model contained ~150,000 variables in the cost function and ~190,000 constraints, requiring 6 hours of computation with a 2.3 GHz processor.

Since the objective here is only to demonstrate typical model output and utility, the particular parameters are not critical. The *type* of information conveyed by the model output, however, is important in establishing SEXPOT's ability to address the questions identified in Section 1:

- 1) *Where* are the best places to exploit renewable power resources?
- 2) *How* can these resources be spatially and temporally integrated into power systems?

Together, the results presented in Figures 7 through 12 (below) illustrate this ability.

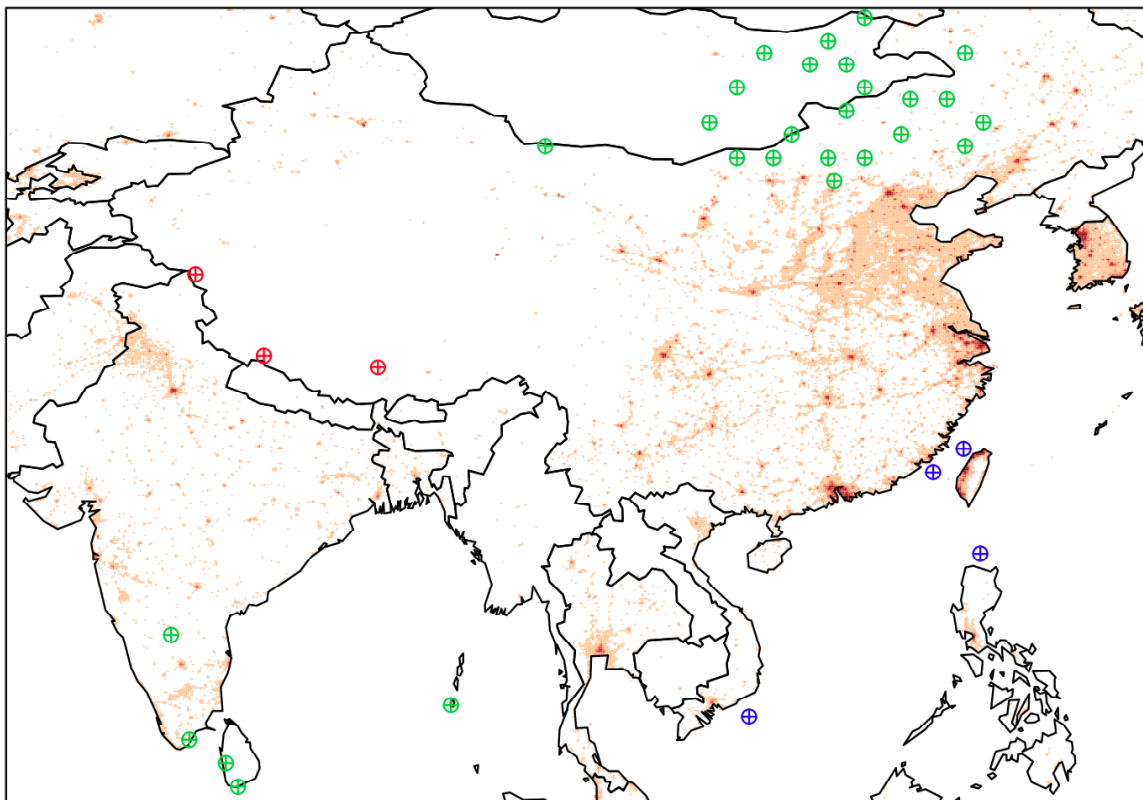
---

<sup>11</sup> When modeling a future period, it is necessary to place realistic constraints on the expansion of hydroelectric power. Hydroelectricity use is unlikely to be influenced by mitigation efforts; given its low cost in suitable locales, it will be built (or not built) regardless. Reflecting this, there is comparatively little variation in global hydro capacity in 2035 across IEA emissions scenarios. SEXPOT assumes a set percentage growth in capacity over the next 25 years, varying by country or region according to the EIA's IEO 2010 projections (which is very similar to the IEA "New Policies" scenario). Globally, this amounts to a ~70% increase in capacity, the majority in China and Latin America. The annual capacity factor constraint (Section 2.7) is unchanged.

Figure 7 shows the location of renewable power generating sites in Asia included in the cost-minimizing LP solution. They are presented against a background of current annual electricity consumption to give an idea of proximity to demand centers. The figure provides two particularly interesting pieces of information: First, when presented with the option of utilizing wind and solar resources (both rooftop and utility-scale) from across the whole of China, the LP model clearly prefers wind power sites in northern China and Mongolia (i.e. they are lower cost). Second, though not apparent in this particular figure, the utility PV sites identified on the Tibetan Plateau are used to provide electricity to northern India. The optimization process determined that greater efficiency offered by sites in China more than offset the additional cost of transmission, compared to lower-quality solar resources in northwest India. In Section 4, I suggest how this kind of information can be used to study the geopolitical implications of renewable power.

Figure 7: SEXPOT output showing renewable power sites in Asia

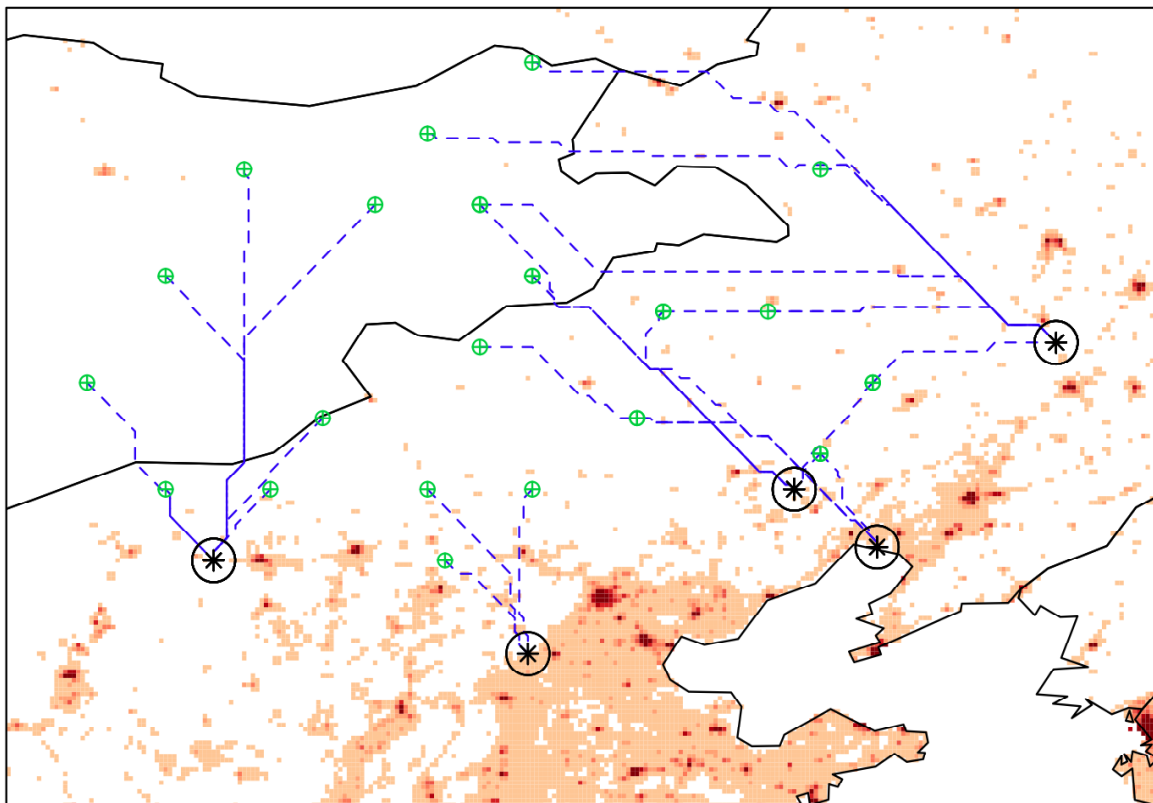
Circles denote utility-scale solar power (red); onshore wind (green); and offshore wind (blue). The background shows the intensity of current electricity consumption (orange-red).



SEXPOT links the sites in Figure 7 to demand centers (i.e. consumption nodes) via transmission lines routed along the shortest topographical path. Figure 8 shows the transmission lines used to link the wind farms in northeast China and Mongolia to urban areas. Note how the lines do not necessarily follow straight paths, as the routing algorithm prevents construction in unsuitable areas and prioritizes open, flat terrain. In some cases, the transmission lines from multiple wind power sites converge to produce high-capacity “corridors”. In other cases, a single generating site is linked to multiple consumption zones, effectively “sharing” power output over time and sending it where it is most needed. Since transmission infrastructure requires coordination and long-term planning, this kind of information can help understand where the most useful linkages are likely to be found.

Figure 8: SEXPOT output showing transmission lines in northeast China and Mongolia

Wind farms (green) are linked to consumption nodes (starred circles) via transmissions lines (blue). The background shows the intensity of current electricity consumption (orange-red).



Aggregated results for a given consumption zone reveal the least-cost mix of technologies over the course of a year. Figure 9 shows results for the southeast U.S. consumption zone, where hydroelectric capacity combines with onshore and offshore wind power to practically eliminate emissions under average operating conditions. The charts show the contribution of each generating technology to meeting mean demand over the course of an average day in each of four seasons.

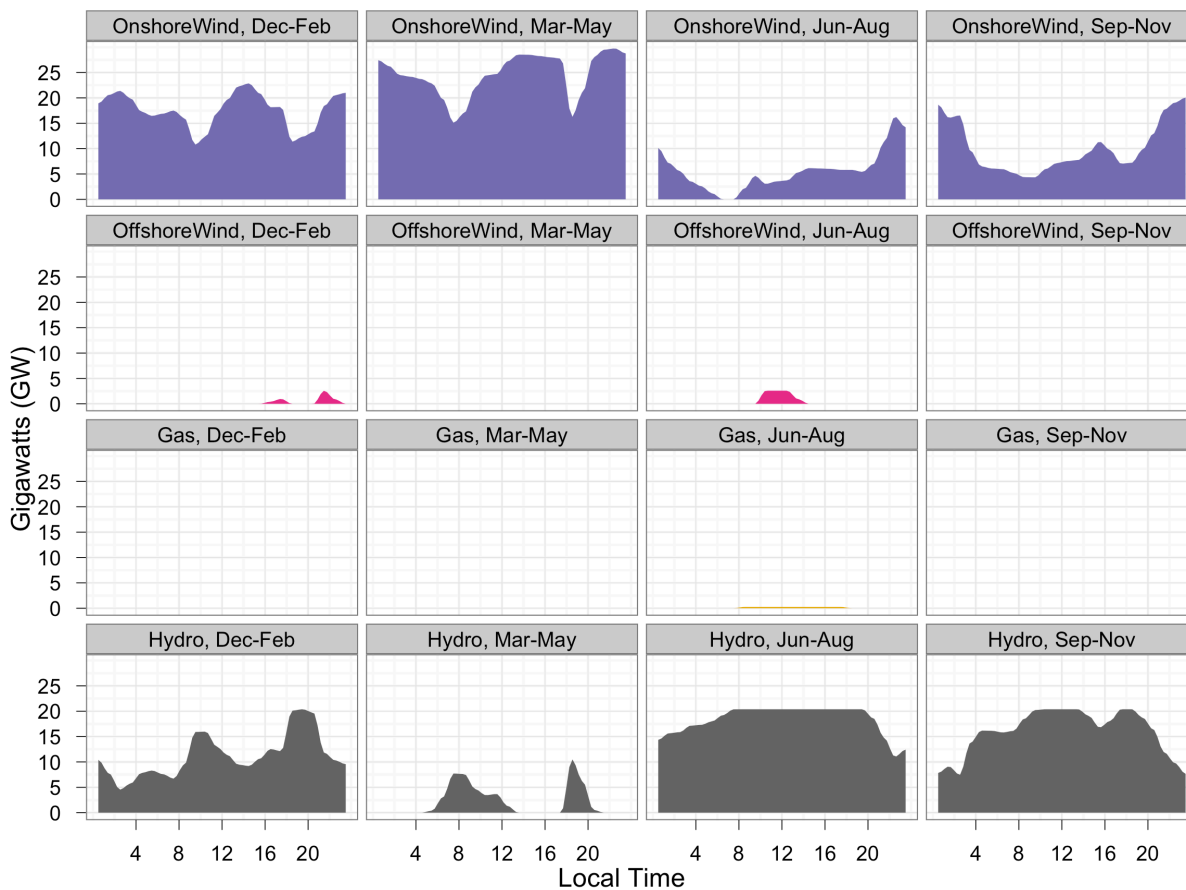
Figure 9: Summary of SEXPOT output for southeast U.S.<sup>12</sup>



<sup>12</sup> Figures 9 through 12 are generated with the *ggplot2* package (Wickham 2009).

Figure 10 presents the same information in a disaggregated view, making it easier to see temporal trends in the contribution of individual technologies. There is a clear drop-off in wind power during summer and fall, which is covered by increased hydroelectric output. One can also see mid-morning and mid-afternoon drops in wind power in winter and spring, again compensated by increased hydroelectric output.

Figure 10: Disaggregated view of SEXPOT output for southeast U.S.



Figures 11 and 12 provide similar model output for the northern India consumption zone. In this case, utility-scale PV power provides a significant contribution during daylight hours. This output also illustrates the consequences of a lack of ramp- or turndown- rate constraints on coal power plants and spatial limits to gas utilization (Section 2.7). If these two factors were appropriately modeled, it's likely the coal and gas contributions in the northern India consumption zone would be significantly different.



Figure 11: Summary of SEXPOT output for northern India

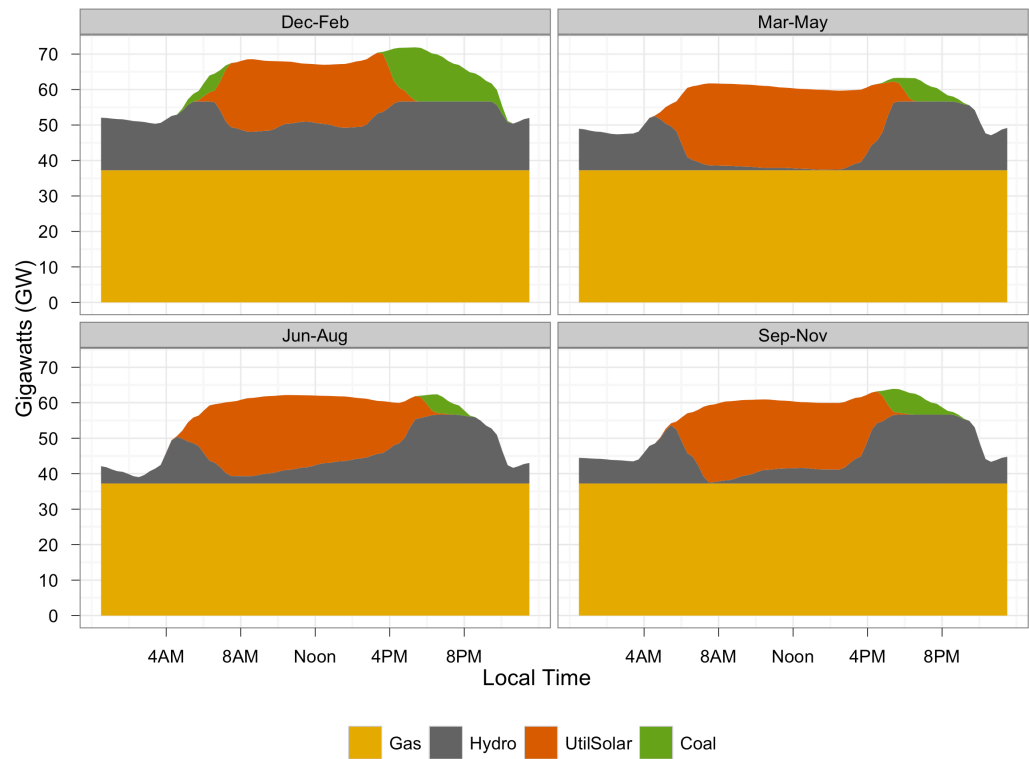
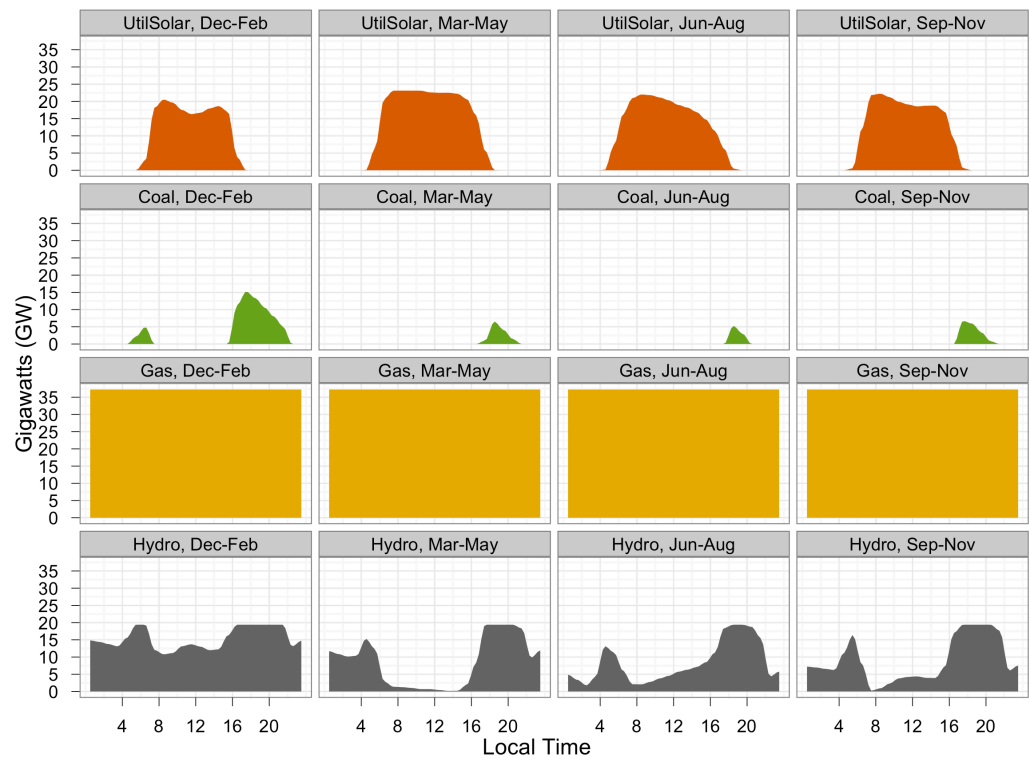


Figure 12: Disaggregated view of SEXPOT output for northern India



#### 4. POTENTIAL APPLICATIONS AND IMPROVEMENTS

In this section, I “think big” about how SEXPOT could be used to address a varied set of research questions. In the process, I outline potential model improvements that would be particularly useful.

SEXPOT’s most obvious use is to identify the particular renewable power technologies and sites that are likely to offer the greatest benefits in a given country or region (i.e. meeting demand or achieving an emissions reduction at minimal additional cost). The basic functionality needed to do is already in place, as shown in Section 3. More realistic analysis, however, needs to consider potential cost reductions over time as renewable technologies respond to learning and economies of scale (Neij 2008). This calls for a longitudinal (multi-period) application of SEXPOT that links a series of single-year model runs and uses the output from each run as input data to the subsequent run. It also requires a more realistic treatment of fossil fuel costs, either by assuming a fuel price trend over time or embedding price elasticities that alter initial assumptions in response to aggregate fuel use in the previous period.

Though wind and solar are the dominant renewable resources worldwide, others may be optimal in particular locales. In theory, there is no reason why technologies like geothermal, wave, tidal, deepwater wind, or concentrating solar power cannot be incorporated into SEXPOT (though data availability is a practical barrier in some cases). And it is not necessary to limit inclusion to renewable technologies. A particularly interesting case is carbon capture and storage (CCS), which exhibits strong spatial-dependency; highly-compressed CO<sub>2</sub> can only be stored in certain geological formations that may not be located close to emission sources. Explicitly modeling the spatial implications could help estimate the realistic potential of CCS to contribute to long-term mitigation.

It may be possible to treat hydroelectric power in a spatially-explicit manner as well. As mentioned in Section 2.7, the generating potential of large dams depends on seasonal variations in water inflow and downstream demand (particularly for irrigation). The quality of global hydrological datasets with related information is steadily improving, as evidenced by the recent

update of the Global Reservoir and Dam (GRanD) database (Lehner et al. 2011). It should be possible to provide basin- and season-specific representation of large hydroelectric dams in the future, and SEXPOT provides a modeling environment in which to embed and make sense of this information. One particularly relevant question concerns the effect of climate change on hydroelectric output and its overall impact on power system operation and costs. A spatial hydroelectric component within SEXPOT, combined with climate model output, could address this question.

With respect to global GHG mitigation, SEXPOT is primarily helpful in identifying deployment patterns that are optimal *from a global perspective*. Clearly, countries design energy policies with many objectives in mind, and GHG mitigation is only one of them. But it still useful (or, at least, provocative) to know the extent to which countries' actions accord with SEXPOT's notion of a socially-optimal approach to GHG reduction. Consider, for example, that the world's largest PV power plant is located in Ontario, a place with neither exceptional solar resources nor a particularly dirty power sector; the plant was built there, because the government of Ontario offers a generous feed-in tariff. If those resources were instead used to construct a plant in, say, South Africa, how many more tons of CO<sub>2</sub> could be averted? Governments will and should use their resources to achieve multiple objectives at home and abroad, but if energy policies swerve radically away from what is in the long-term interest of the planet, this should be stated plainly. SEXPOT provides a means of identifying such situations.

At present, SEXPOT places no constraints on the geographic sourcing of renewable power; if the LP model deems Chinese or Pakistani solar power to be the most cost-effective means of meeting Indian demand, it will build a transmission line. The model could be configured, however, to test the consequences of full, partial, or limited power transfer between particular countries or regions. In some cases, prioritizing national energy security or geopolitical factors may have little effect on the cost of GHG abatement. If domestic renewable resources are subpar, however, the cost of forgoing superior foreign resources could be significant. SEXPOT could be used to address these geopolitical questions surrounding renewable energy, perhaps identifying transnational transmission projects or trading opportunities with long-term benefits.

An unaddressed issue throughout this thesis is that of uncertainty. Modeling large-scale systems over time is always subject to significant error. There is uncertainty in the wind and solar data, the capital and fuel cost assumptions, and the electricity prediction model, among other aspects. Serious application of SEX POT will need to address these concerns by conducting probabilistic analyses (e.g. Monte Carlo techniques) to determine the extent to which model conclusions are sensitive to input uncertainty. This will require SEX POT simulations to be run thousands of times with different model assumptions. The computational demands are extreme, but utilizing “cloud computing” resources offer a comparatively low-cost solution. If SEX POT can be successfully spawned across a thousand virtual machines via the cloud, large-scale uncertainty analysis could be carried out in relatively short order.

Finally, SEX POT’s modeling approach could be used to assess the consequences of broad changes to electricity *consumption* patterns. The cost and technical feasibility of integrating renewable power is largely determined by the extent to which temporal trends in generator output and consumption overlap. Altering patterns of electricity consumption, either through investment in energy efficiency, electrification of the transportation fleet, or a wider set of demand side management (DMS) tools, can affect this relationship (Moura and de Almeida 2010). By testing alternative load profiles within SEX POT, it may be possible to identify which DMS interventions are most useful in different locales and where it makes the most economic and climatic sense to focus on energy efficiency.

## 5. CONCLUSION

This thesis introduced the Spatiotemporally-Explicit Power and Transmission (SEXPOT) computer model for simulating the deployment of renewable power technologies. SEXPOT evaluates wind and solar power potential across large areas of the world, utilizing global geophysical and socioeconomic data and a moderate-complexity linear programming model to provide low-cost, high-resolution analysis. Model output reveals the preferred locations of wind farms, solar power plants, and transmission lines and shows how variable power sources can be integrated with conventional technologies to meet demand hour-by-hour. Simulations can be configured to identify least-cost deployment strategies in the presence of emissions constraints and/or renewable generation targets.

A model run simulating a global mitigation scenario in 2035 was used to illustrate SEXPOT's capabilities. The results reveal the model's ability to provide information relevant to two key questions: 1) *Where* are the best places to exploit renewable power resources? and 2) *How* can these resources be spatially and temporally integrated into power systems? For example, the illustrative model run revealed wind power sites in northern China and Mongolia to be economically preferable to wind and solar resources elsewhere in China and identified feasible transmission routes for connecting those sites to northeast consumption centers.

Hourly model output showed how multiple technologies can be combined to meet electricity demand over the course of a year in a given market. Results for the southeast U.S. suggested emissions could be practically eliminated by utilizing hydroelectric power to accommodate seasonal and diurnal fluctuation in onshore wind power generation. SEXPOT's integration of spatiotemporal data over large areas makes it an ideal tool for identifying opportunities to "mix and match" spatially-disparate resources to smooth fluctuations in power supply and reduce the cost of accommodating renewable power.

Though only a prototype with much room for improvement, SEXPOT shows promise as a tool for addressing practical research questions. Potential applications were identified in a variety of areas, ranging from the economics of GHG mitigation to geopolitics and infrastructure planning.

Utilizing SEXPOT in these ways will require further development of data and techniques. In particular, the performance of conventional generating technologies, especially hydroelectricity, needs to be better specified. And modifying SEXPOT to run as a multi-period model over many decades would allow a more realistic treatment of long-term deployment potential and costs.

As countries seek to realize the benefits of large-scale renewable power, anticipating barriers and identifying bold, yet-unimagined opportunities is increasingly important. A renewables-based future will require intelligent harvesting of energy resources that are free, clean, and plentiful but also dispersed and variable. Spatiotemporally-explicit modeling tools like SEXPOT help reveal how these resources can be utilized most effectively. Such efforts can lower the cost of a transition to renewable energy, ultimately helping to address widespread concerns like energy security, air pollution, and global climate change.

## REFERENCES

- Aboumahboub, T., Schaber, K., Tzscheuschler, P., and Hamacher, T. 2010. Optimization of the utilization of renewable energy sources in the electricity sector. *Proceedings of the 5th IASME/WSEAS International Conference on Energy and Environment*: 196-204.
- Amante, C. and Eakins, B.W., 2009. ETOPO1 1 arc-minute global relief model: procedures, data sources and analysis. NOAA Technical Memorandum NESDIS NGDC-24, March.
- Amaral, S., Camara, G., Monteiro, A.M.V., Quintanilha, J.A., and Elvidge, C.D. 2005. Estimating population and energy consumption in Brazilian Amazonia using DMSP night-time satellite data. *Computers, Environment and Urban Systems* 29 (2): 179-195.
- Blair, N., Short, W., and Heimiller, D. 2005. Reduced form of detailed modeling of wind transmission and intermittency for use in other models. Presented at WindPower 2005 Conference, Denver, Colorado. 15-18 May.
- Bontemps, S., Defourney, P. and van Bogaert, E. 2010. GLOBCOVER 2009: products description and validation report. European Space Agency and Université catholique de Louvain.
- Chand, T.R.K., Badarinath, K.V.S., Elvidge, C.D., and Tuttle, B.T. 2009. Spatial characterization of electrical power consumption patterns over India using temporal DMSP-OLS night-time satellite data. *International Journal of Remote Sensing* 30 (3): 647-661.
- Connolly, D., Lund, H., Mathiesen, B.V., and Leahy, M. 2010. A review of computer tools for analysing the integration of renewable energy into various energy systems. *Applied Energy* 87: 1059-1082.
- Czisch, G. 2006a. Realisable scenarios for a future electricity supply based 100% on renewable energies. Unpublished manuscript. Available at: [http://130.226.56.153/rispubl/reports/ris-r-1608\\_186-195.pdf](http://130.226.56.153/rispubl/reports/ris-r-1608_186-195.pdf)
- Czisch, G. 2006b. Joint renewable electricity supply for Europe and its neighbors. Unpublished manuscript. Available at: [http://www.iset.uni-kassel.de/abt/w3-w/projekte/RenElSupEU\\_Trans\\_ot\\_WR+Ch.pdf](http://www.iset.uni-kassel.de/abt/w3-w/projekte/RenElSupEU_Trans_ot_WR+Ch.pdf)
- Deutch, J.M., Forsberg, C.W., Kadak, A.C., Kazimi, M.S., Moniz, E.J., Parsons, J.E., Yangbo, D., and Pierpoint, L. 2009. Update of the MIT 2003 future of nuclear power. Massachusetts Institute of Technology Energy Initiative. Available at: <http://web.mit.edu/nuclearpower/pdf/nuclearpower-update2009.pdf>
- Dijkstra, E.W. 1959. A note on two problems in connexion with graphs. *Numerische Mathematik* 1: 269-271.
- DoE. 2008. 20% wind energy by 2030: increasing wind energy's contribution to U.S. electricity supply. U.S. Department of Energy, DOE/GO-102008-2567, July.
- EEA. 2009. Europe's onshore and offshore wind energy potential. European Environmental Agency, Technical Report No. 6/2009, Copenhagen.
- EIA. 2010. Updated capital cost estimates for electricity generation plants. U.S. Energy Information Administration, Office of Energy Analysis, Washington.
- Elliott, D. L., C. G. Holladay, W. R. Barchet, H. P. Foote, and W. F. Sandusky, Wind Energy Resource Atlas of the United States, DOE/CH 10093-4, Natl. Renew. Energy Lab., Golden, Colo., 1986.
- EnerNex. 2010. Eastern wind integration and transmission study. Prepared for the National Renewable Energy Laboratory. Subcontract report NREL/SR-550-47078.

- FAO, IIASA, ISRIC, ISSCAS, and JRC. 2009. Harmonized world soil database (version 1.1). Food and Agriculture Organization, Rome, Italy and International Institute for Applied Systems Analysis, Laxenburg, Austria.
- Faraji-Zonooz, M.R., Nopiah, Z.M., Yusof, A.M., and Sopian, K. 2009. A review of MARKAL energy modeling. *European Journal of Scientific Research* 26 (3): 352-361.
- Feinberg, E.A. and Genethliou, D. 2005. Load forecasting. In *Applied Mathematics for Restructured Electric Power Systems*, ed. J.H. Chow, F.F. Wu, and J. Momoh, 269-285. Springer: United States.
- Friedman, J.H. 1991. Multivariate adaptive regression splines. *Annals of Statistics* 19: 1-141.
- GE Energy. 2010. Western wind and solar integration study. Prepared for the National Renewable Energy Laboratory. Subcontract report NREL/SR-550-47434.
- Gilman, P., Blair, N., Mehos, M., Christensen, C., Janzou, S., and Cameron, C. 2008. Solar advisor model user guide for version 2.0. Technical Report No. TP-670-43704, National Renewable Energy Laboratory, Golden, Colorado.
- Hadjipaschalis, I., Poullikkas, A., and Efthimiou, V. 2009. Overview of current and future energy storage technologies for electric power applications. *Renewable and Sustainable Energy Reviews* 13 (6-7): 1513-1522.
- Hahn, H., Meyer-Neiberg, S., and Pickl, S. 2009. Electric load forecasting methods: tools for decision making. *European Journal of Operational Research* 199: 902-907.
- Hijmans, R.J. and van Etten, J. 2011. raster: Geographic analysis and modeling with raster data. R package version 1.8-15. Available at: <http://CRAN.R-project.org/package=raster>
- IEA. 2010. World energy outlook 2010. International Energy Agency, Paris.
- IUCN and UNEP. 2010. World database on protected areas (WDPA). International Union for Conservation of Nature and United Nations Environment Programme (World Conservation Monitoring Centre), Cambridge, United Kingdom.
- Izquierdo, S., Rodrigues, M., and Fueyo, N. 2008. A method for estimating the geographical distribution of the available roof surface area for large-scale photovoltaic energy-potential evaluations. *Solar Energy* 82: 929-939.
- Jackson, T.L., Feddema, J.J., Oleson, K.W., Bonan, G.B., and Bauer, J.T. 2010. Parameterization of urban characteristics for global climate modeling. *Annals of the Association of American Geographers* 100 (4): 848-865.
- Keitt, T.H., Bivand, R., Pebesma, E., and Rowlingson, B. 2010. rgdal: bindings for the geospatial data abstraction library. R package version 0.6-33. Available at: <http://CRAN.R-project.org/package=rgdal>
- King, D.L., Gonzalez, S., Galbraith, G.M., and Boyson, W.E. 2007. Performance model for grid-connected photovoltaic inverters. Sandia National Laboratories, Albuquerque, New Mexico.
- Konis, K. 2011. lpSolveAPI: R interface for lp\_solve version 5.5.2.0. R package version 5.5.2.0-1. Available at: <http://CRAN.R-project.org/package=lpSolveAPI>
- Kourzeneva, E. 2009. Global dataset for the parameterization of lakes in numerical weather prediction and climate modeling. ALADIN Newsletter 37, F. Bouttier and C. Fischer, Eds., Météo-France, Toulouse, France, 46-53.
- Kourzeneva, E. 2010. External data for lake parameterization in numerical weather model prediction and climate modeling. *Boreal Environment Research* 15: 165-177.
- Kusiak, A., Zheng, H., and Song, Z. 2009. On-line monitoring of power curves. *Renewable Energy* 34: 1487-1493.



- Lehner, B. and Döll, P. 2004. Development and validation of a global database of lakes, reservoirs, and wetlands. *Journal of Hydrology* 296 (1-4): 1-22.
- Lehner, B., Liermann, C.R., Revenga, C., Vörösmarty, C., Fekete, B., Crouzet, P., Döll, P., Endejan, M., Frenken, K., Magome, J., Nilsson, C., Robertson, J.C., Rödel, R., Sindorf, N., and Wisser, D. 2011. Global reservoir and dam (GRanD version 1.1) database technical documentation. Available at: [http://www.gwsp.org/fileadmin/downloads/GRanD\\_Technical\\_Documentation\\_v1\\_1.pdf](http://www.gwsp.org/fileadmin/downloads/GRanD_Technical_Documentation_v1_1.pdf)
- Letu, H., Hara, M., Yagi, H., Tana, G., and Nishio, F. 2009. Estimating the energy consumption with nighttime city light from the DMSP/OLS imagery. Presented at Urban Remote Sensing Joint Event, 20-22 May, Shanghai, China.
- Lu, X., McElroy, M.B., and Kiviluoma, J. 2009. Global potential for wind-generated electricity. *Proceedings of the National Academy of Sciences* 106 (27): 10933-10938.
- McElroy, M.B., Lu, X., Nielsen, C.P., and Wang, Y. 2009. Potential for wind-generated electricity in China. *Science* 325: 1378-1380.
- Menicucci, D.F. 1986. Photovoltaic array performance simulation models. *Solar Cells* 18: 383-392.
- Milborrow, S. 2011. earth: multivariate adaptive regression spline models. R package version 2.6-2. Available at: <http://CRAN.R-project.org/package=earth>
- Moura, P.S. and de Almeida, A.T. 2010. Multi-objective optimization of a mixed renewable system with demand-side management. *Renewable and Sustainable Energy Reviews* 15 (5): 1461-1468.
- Nelson, A. 2008. Estimated travel time to the nearest city of 50,000 or more people in year 2000. Global Environmental Monitoring Unit, Joint Research Centre of the European Commission, Ispra, Italy. Available at: <http://bioval.jrc.ec.europa.eu/products/gam>
- Neij, L. 2008. Cost development of future technologies for power generation – a study based on experience curves and complementary bottom-up assessments. *Energy Policy* 36 (6): 2200-2211.
- NOAA. 2009. DMSP-OLS nighttime lights time series (1992-2008). Image and data processed by the National Oceanic and Atmospheric Administration's National Geophysical Data Center; DMSP data collected by U.S. Air Force Weather Agency. Available at: <http://www.ngdc.noaa.gov/dmsp/downloadV4composites.html>
- O'Connor, R., Reed, G., Mao, Z., and Jones, A.K. 2010. Improving renewable resource utilization through integrated generation management. Presented at the Power and Energy Society General Meeting (IEEE), Minneapolis, 25-29 July.
- ORNL. 2008. LandScan™ 2008 global population dataset. Oak Ridge National Laboratory, Oak Ridge, Tennessee.
- Perpinan, O. 2011. solar: calculation of solar radiation and PV systems. R package version 0.23. Available at: <http://CRAN.R-project.org/package=solar>
- R Core Development Team. 2011. R: a language and environment for statistical computing. R Foundation for Statistical Computing, Vienna, Austria. Available at: <http://www.R-project.org/>
- Reinecker, M.M., Suarez, M.J., Todling, R., Bacmeister, J., Takacs, L., Liu, H.-C., Gu, W., Sienkiewicz, M., Koster, R.D., Gelaro, R., Stajner, I., and Nielsen, J.E. 2008. The GEOS-5 Data Assimilation System – documentation of versions 5.0.1, 5.1.0, and 5.2.0. Technical Report Series on Global Modeling and Data Assimilation, Volume 27. National Aeronautics and Space Administration.

- Ridley, B., Boland, J., and Lauret, P. 2010. Modelling of diffuse solar fraction with multiple predictors. *Renewable Energy* 35: 478-483.
- Short, W. 2007. Regions in energy market models. Technical Report NREL/TP-640-40506, National Renewable Energy Laboratory, Golden, Colorado.
- Short, W., Blair, N., Sullivan, P., and Mai, T. 2009. ReEDS model documentation: base case data and model description. National Renewable Energy Laboratory, Golden, Colorado.
- Stott, B. and Marinho, J.L. 1979. Linear programming for power-system network security applications. *Power Apparatus and Systems* 98 (3): 837-848.
- Sullivan, P., Logan, J., Bird, L., and Short, W. 2009. Comparative analysis of three proposed federal renewable electricity standards. Technical Report NREL/TP-6A2-45877, National Renewable Energy Laboratory, Golden, Colorado.
- Svenningsen, L. 2010. Proposal of an improved power curve correction. Presented at the European Wind Energy Conference and Exhibition, Warsaw, Poland. 20-23, April.
- Ummel, K. 2010a. Concentrating solar power in China and India: a spatial analysis of technical potential and the cost of deployment. Working Paper 219, Center for Global Development, Washington.
- Ummel, K. 2010b. Global prospects for utility-scale solar power: toward spatially explicit modeling of renewable energy systems. Working Paper 235, Center for Global Development, Washington.
- UNEP. 2010. Global trends in sustainable energy investment 2010 report. United Nations Environment Programme and Bloomberg New Energy Finance. Available at: <http://sefi.unep.org/english/globaltrends2010.html>
- van Etten, J. 2011. gdistance: distances and routes on geographical grids. R package version 1.1-1. Available at: <http://CRAN.R-project.org/package=gdistance>
- Verdin, K.L., Godt, J.W., Funk, C., Pedreros, D., Worstell, B., and Verdin, J. 2007. Development of a global slope dataset for estimation of landslide occurrence resulting from earthquakes. United States Geologic Survey, Colorado, Open-File Report 2007-1188.
- Wheeler, D. and Ummel, K. 2008. Calculating CARMA: global estimation of CO2 emissions from the power sector. Working Paper 145, Center for Global Development, Washington.
- Wickham, H. 2009. *ggplot2: elegant graphics for data analysis*. Springer, New York.

## APPENDIX A. DERIVATION OF METEOROLOGICAL INPUTS

### A.1 WIND SPEED

GEOS-5 model output provides hourly wind speed at 2, 10, and 50 m above displacement height. Wind speed typically increases with height, and the observed correlation is approximated well by a power law relationship (Elliott et al. 1986):

$$V_z = V_r \left( \frac{z}{r} \right)^\alpha$$

where  $V_z$  and  $V_r$  are wind speeds at effective heights  $z$  and  $r$ , and  $\alpha$  is a scaling coefficient determined from at least two observations along the vertical wind profile (Archer and Jacobsen 2005):

$$\alpha = \frac{\sum_{i=1}^2 \ln\left(\frac{V_i}{V_r}\right) \ln\left(\frac{z_i}{r}\right)}{\sum_{i=1}^2 \ln\left(\frac{z_i}{r}\right)^2}$$

The three GEOS-5 observations are used to calculate the best-fit  $\alpha$ , which is then used to extrapolate (or, in some cases, interpolate) from 50 m above displacement height to the desired hub heights of 80 and 120 m above the surface. Because GEOS-5 wind speed is relative to the displacement height and not the surface, the  $r$  term in Eq. 1 and 2 is adjusted to reflect the cell-specific mean monthly displacement height within the model (effectively the height of predominant vegetation).

### A.2 SOLAR IRRADIANCE

GEOS-5 output includes estimated total surface irradiance on a horizontal plane (i.e. “global horizontal irradiance”, GHI) for each hour. Calculating the effective irradiation on a fixed-tilted or sun-tracking PV array requires that the GHI be deconstructed into direct and diffuse components. A comparatively new algorithm is used here (the “BRL model”), which initial assessments suggest provides better prediction of the direct component across a range of locales (Ridley et al. 2010). The BRL model is based on an observed sigmoid relationship between the widely used “clearness index” and the diffuse fraction of GHI, with additional predictor variables introduced to improve the model fit.

For hour  $t$ , the BRL model predicts the diffuse fraction ( $d$ ) of GHI by:

$$d = \frac{1}{1 + e^{-5.38 + 6.63k_t + 0.006AST - 0.007\alpha + 1.75K_t + 1.31\psi}}$$

where  $k_t$  is the hourly clearness index (ratio of GHI to extraterrestrial radiation),  $AST$  is the apparent solar time,  $\alpha$  is the solar angle,  $K_t$  is the daily clearness index, and  $\psi$  is a “persistence” indicator given by:

$$\psi = \begin{cases} \frac{k_{t-1} + k_{t+1}}{2} & \text{sunrise} < t < \text{sunset} \\ k_{t+1} & t = \text{sunrise} \\ k_{t-1} & t = \text{sunset} \end{cases}$$

The remaining predictors are obtainable by standard astronomical calculations, taking into account location, time and date.

The *solaR* package implements the BRL model and executes all necessary angular calculations, taking into account the tilt of panels in either fixed (rooftop) or single-axis tracking (utility) applications. A system optimization function within *solaR* is used to calculate the optimal fixed-tilt angle for a sample of sites globally. This is then spatially interpolated and used to provide the optimal tilt when calculating effective irradiance for all feasible sites. A similar procedure is used to determine the optimal row spacing for utility-scale facilities using a single-axis “backtracking” array. The resulting output is the effective irradiance on the generator plane for each hour.

### A.3 AIR DENSITY AND RELATIVE HUMIDITY

Air density and relative humidity are not provided directly in GEOS-5 output but are approximated using ambient temperature and specific humidity. Air density ( $D$ ) is used in the wind turbine efficiency model; relative humidity ( $RH$ ) for hourly electricity load prediction.

$RH$  is given by the ratio of vapor pressure ( $E$ ) to the saturation vapor pressure ( $E_s$ ),

$$RH = \frac{E}{E_s}$$

where  $E_s$  is approximated by

$$E_s = 6.11 \left[ 10^{\frac{7.5T_c}{(237.7+T_c)}} \right]$$

and  $E$  is defined by a relationship with specific humidity ( $SH$ ) and atmospheric pressure ( $P$ ),

$$\frac{SH}{1 - SH} = \frac{0.622E}{P - E} \Rightarrow E = \frac{P(SH)}{0.378SH + 0.622}$$

where  $P$  is estimated by way of an approximation of air density ( $D$ ) using ambient temperature ( $T_c$ ) and elevation ( $Z$ ) as inputs.

$$D = \frac{101,325}{287(T_c + 273.15)} e^{\frac{-9.8Z}{(T_c + 273.15)}}$$

$$P = \frac{287D(T_c + 273.15)}{100}$$

## APPENDIX B. TECHNOLOGY PERFORMANCE MODELS

### B.1 WIND TURBINE

The net instantaneous power output ( $P$ ) of a wind turbine with rated power  $P_r$  is given by:

$$P = P_r C_p \eta_{m,el}$$

where  $\eta_{m,el}$  is mechanical and electrical efficiency (assumed to be 90%) and  $C_p$  is the instantaneous power coefficient. For a pitch-controlled turbine,  $C_p$  is commonly approximated by a piecewise function that is parabolic over the middle range (Pallabazzer 2004):

$$C_p = \begin{cases} 0 & V < V_i \\ \frac{V^2 - V_i^2}{V_r^2 - V_i^2} & V_i \leq V \leq V_r \\ 1 & V_r < V \leq V_c \\ 0 & V > V_c \end{cases}$$

where  $V$  is the instantaneous wind speed,  $V_i$  is the cut-in wind speed,  $V_r$  is the rated wind speed, and  $V_c$  is the cut-out wind speed, as provided by the turbine manufacturer.

An alternative is developed here to better reflect the actual shape of reported power curves, which suggest the relationship of  $C_p$  to  $V$  resembles a logistic rather than parabolic function over the mid-section. The functional form is drawn from Kusiak et al. (2009), but it is modified to force  $C_p=0$  when  $V=V_i$ , as defined above. Four parameters ( $\alpha$ ,  $\beta$ ,  $A$ , and  $B$ ) are required to fully specify the mid-section of the power curve. Because the asymptotic value may exceed unity,  $C_p$  is restricted to a maximum value of 1:

$$C_p = \min \left[ \alpha \frac{1 + (AV_{scl} - 1)e^{-\frac{V_{scl}}{\beta}}}{1 + Be^{-\frac{V_{scl}}{\beta}}}, 1 \right]$$

where wind speed  $V$  within the range  $V_i \leq V \leq V_r$  is scaled such that:

$$V_{scl} = \frac{V - V_i}{V_r - V_i}$$

Fully specified manufacturer power curves for 30 large-scale turbines ranging from 810 kW to 7,500 kW (median = 1500 kW) were obtained from NREL's System Advisor Model (SAM; Gilman et al. 2008). The power curve equation was fit to these data using a non-linear least squares estimator to determine optimal parameter values ( $\alpha = 1.066$ ,  $\beta = 0.157$ ,  $A = 10.782$ , and  $B = 44.904$ ).

The reference power curve characteristics ( $V_{x,ref}$ ) assume a reference air density ( $\rho_{ref}$ ), typically 1.225 kg per m<sup>3</sup> at sea level. Given actual air density ( $\rho_{site}$ ), site- and time-specific performance characteristics ( $V_{x,site}$ ) are derived for use in the power curve equation (Svenningsen 2010):

$$V_{x,site} = V_{x,ref} \begin{cases} V_{x,ref} < 7 \text{ ms}^{-1} & \kappa^{\frac{1}{3}} \\ 7 \text{ ms}^{-1} \leq V_{x,ref} \leq 13 \text{ ms}^{-1} & \kappa^{\frac{1}{-0.25(V_{x,ref} - 7) + 3}} \\ V_{x,ref} > 13 \text{ ms}^{-1} & \kappa^{\frac{2}{3}} \end{cases}$$

where  $\kappa$  is the ratio of the reference air density to actual air density, using the approximation for the latter in Appendix A.3.

## B.2 PHOTOVOLTAIC (PV) ARRAY

The alternating current output of a PV array ( $P_{AC}$ ) is a function of incident radiation ( $E_{inc}$ ), module efficiency ( $\eta_{mod}$ ), inverter efficiency ( $\eta_{inv}$ ), and miscellaneous derate losses ( $\eta_{derate}$ ):

$$P_{AC} = E_{inc} \eta_{mod} \eta_{inv} \eta_{derate}$$

Menicucci (1986) provides a simple model to estimate instantaneous module efficiency as a function of incident radiation, cell temperature ( $T_{cell}$ ), and module efficiency ( $\eta_{mod,ref}$ ) at the reference cell temperature ( $T_{ref}$ ):

$$\eta_{mod} = \begin{cases} E_{inc} \geq 100 \text{ Wm}^{-2} & \eta_{mod,ref} \left[ 1 + \gamma (T_{cell} - T_{ref}) \right] \\ E_{inc} < 100 \text{ Wm}^{-2} & 0.01 (E_{inc}) (\eta_{mod, E_{inc}=100}) \end{cases}$$

Cell temperature is given by:

$$T_{cell} = E_{inc} e^{a+b(w_{10})} + T_a + \left( \frac{E_{inc}}{E_{ref}} \right) \Delta T$$

where wind velocity at 10 m above the surface ( $w_{10}$ ), global irradiance under reference conditions ( $E_{ref}$ ), and ambient temperature ( $T_a$ ) are determinants. The coefficients  $a$ ,  $b$ , and  $\Delta T$  depend upon the module materials and mounting configuration and are determined empirically though testing under reference conditions; module characteristics are provided by SAM. Inverter losses are determined using the techniques and equations in King et al. (2007). The derate losses consist of pre- and post-inverter losses equal to ~9% and ~2%, respectively.